Low and High Resolution Analysis of Nonhuman Primate Reaching Behavior

By

RYAN NORTH
DISSERTATION

Submitted in partial satisfaction of the requirements for the degree of

DOCTOR OF PHILOSOPHY

in

Biomedical Engineering

in the

OFFICE OF GRADUATE STUDIES

of the

UNIVERSITY OF CALIFORNIA

DAVIS

Approved:

Wilsaan Joiner

Jaqueline Bresnahan

Carolynn Patten

Committee in Charge

2022

Acknowledgements

I would first like to thank my advisor Dr. Wilsaan Joiner and my dissertation committee for guiding me through very fluid primate research world on top of both a cross country move closely followed by a worldwide pandemic. You have all taught me a great deal in scientific research, balancing those goals with life and have been supportive through those changes. Additionally, I'd like to thank Drs. Betty Mei and Laurence Bray from West Virginia University and George Mason University respectively for believing in me and giving me the opportunity to start the PhD program.

I'm greatly indebted to the International Primate Consortium and the primate trainers without whom this project would not have been possible. Learning from all of you, from various different fields, has had a tremendous impact upon this project and my future career goals. From the off the wall discussions, to being in the primate room completing the tasks with the animals, this experience cannot be matched and I could not be more thankful.

Lastly, I would like to thank my family and friends who can supported and pushed me through to complete the PhD. You all kept my spirits up when I was feeling down. The late night calls whether it would be Mom, Dad, Lisa or Praneeth kept me going through the night to hit the next milestone. This accomplishment is as much yours as it is mine.

Abstract

The number of people affected by spinal cord injuries (SCI) ranges from 2.5 million to 4 million worldwide. Individuals with cervical SCI commonly experience difficulty in controlling hand function, largely due to a reduced ability to perform individuated finger movements that they may never fully recover. Specifically, impairment in the ability to accurately coordinate skilled hand actions is a well-established deficit of injury (e.g., precision grip between the thumb and index finger). Previous studies in both human and nonhuman primate models of SCI have demonstrated some recovery of these abilities over time through various compensatory pathways and mechanisms, including through neural regrowth or through physical rehabilitation with repetitive behavioral tasks.

Behavioral tasks that require coordinated finger movements are important tools to examine functional recovery and potential effects of treatments after SCI. A tool used to evaluate precision hand gestures in nonhuman primates is the Brinkman board. These boards have surfaces with specially shaped grooves, called wells, that encourage the use of precision grip during a simple reach and grasp task. Performance is scored quantitatively based on gradations of the animal's success or failure. This behavioral data provide an assessment of real-world ability, which can then be correlated with other metrics like neural regrowth. However, the change in ability after SCI may frustrate an animal who was previously able to complete the Brinkman board task with ease; they may not even attempt the task due to the task now being too difficult. Assessments must be challenging enough to be an accurate measure of ability, but a task that's too difficult can cause the animal to give up, not just on the given task but on future similar measures or repeated assessments. Failure to participate with the Brinkman board task for any reason results in the

same completion time score, conflating any distinction between simply not performing the task and trying but failing to complete it.

A **primary objective of this study** is to improve the quality of behavioral data collection by modifying existing Brinkman boards to expand the range and resolution of behavioral performance (floor behavior) for post-SCI animals to complete while providing comparable metrics to existing data. These modified Brinkman boards, Remedial Brinkman boards, were designed to be easier to complete and provide additional opportunities for food rewards to the animal. These additional opportunities in the Remedial Brinkman board task manifested in higher participation and performance in the Standard Brinkman board task, specifically by keeping the animal engaged with the task.

Low resolution quantitative behavioral data collected through the Brinkman board task can be supplemented with a higher resolution quantitative method, such as motion tracking. These quantitative measures of finger movements could provide, higher resolution data that may allow additional insights into functional recovery. However, detailed temporal information of hand movement kinematics during recovery is lacking; there is little information on the precise timecourse during which this control improves. To begin to address this need, unimpaired animals' hands were recorded from multiple angles during completion of the Brinkman board task. These recordings were partially annotated by hand, and then used to train a deep learning algorithm to automatically annotate all future recordings, providing a detailed quantitative measure of performance. These quantitative measures included movement velocity, the size of the aperture between the thumb (D1) and index digit (D2), the temporal relationship between velocity and maximum aperture, and finger

extension of the index digit. Some of these metrics have been seen in previous human and nonhuman primate studies completing reach and grasp tasks.

The **second objective of this study** was to devise a methodology in which behaviors before and after spinal cord injury can be systematically tracked (using high and low resolution quantitative data) in nonhuman primate models, and that could measure changes in their functional abilities.

Table of Contents

List of Figures/Tables

Chapter 1: Modification to the Standard Brinkman board task to better capture low level behavioral performance of hand function

Summary Statement

Non-human primates after spinal cord injury have difficulty completing the Standard Brinkman board task. This has led some animals to disengage with the task. Remedial Brinkman boards, designed to be easier to complete, were implemented within the behavioral testing suite. This increased performance in the Standard Brinkman board task.

Abstract

Non-human primates exhibit difficulties with individuated finger movements after cervical spinal cord injury (SCI). The difficulties are revealed by poor performance on tasks requiring dexterous movements such as the Standard Brinkman board task. This task specifically involves the coordinated movement of their impaired digits to retrieve food rewards from wells (varying in size and orientation). In conversations with animal trainers, it has been observed that some animals refuse to engage with the Standard Brinkman board task, presumably due to a lack of motivation or learned helplessness. To address the resulting gaps in the data, Remedial Brinkman boards were created based upon the Standard Brinkman boards.

Remedial Brinkman boards were designed to be easier to complete than the existing behavioral boards by increasing the well size and sloped edges. This allows for a greater variety of reaching behaviors to be successful in retrieving the food reward. The utility of these boards was determined by tracking spinal cord injury animals whose performance has plateaued. Increased performance is determined by an increase in average score and a decrease in time of completion. Additionally, non-participation metrics such as 0 scores and 60 second timeouts were also

collected. A decrease in the non-participation metrics would also indicate an increase in performance.

Two animals whose performance metrics has plateaued were exposed to Remedial Brinkman boards along with the Standard Brinkman boards. The order of the boards given to the animals was consistent. Only performance metrics on Standard Brinkman boards A and B were collected and used for this study.

Both animals showed a significant improvement in their performance on the Standard Brinkman board A following repeated exposure to the Remedial Brinkman boards. Animal 1's average score improved from 1.08 to 1.96 while Animal 2's average score improved from 0.51 to 1.47. These results suggest that both animals retrieved the food rewards more frequently. Time of completion also decreased in both animals from 55.23 seconds to 24.89 seconds and 54.48 seconds to 35.27 seconds, respectively. This improvement can be seen in the decrease in non-participation metrics, namely a decrease in 0 scores and timeouts. Both animals saw a significant increase in average score for Brinkman board B but not time of completion. This suggests that the animals participated more regularly but may not physically be able to collect the food rewards before timeout. This would indicate their true peak performance as the animals are participating in the Standard Brinkman board task but unable to complete it within the allotted time.

Introduction

Individuals with cervical spinal cord injury (SCI) commonly experience difficulty in upper extremity control and hand function, largely due to a reduced ability to perform gross and fine movements (i.e., accurately coordinated finger movement). As of 2019, over 17000 new spinal cord injuries are recorded in the United States as reported by the Department of Veteran Affairs [1]. The most common SCI is an incomplete spinal cord injury at the cervical level, more specifically damage to the cortical spinal tract that conveys voluntary motor function, which largely attributes to the difficulties in fine movements [1], [2].

Previous studies in both human and nonhuman primate models of SCI have demonstrated recovery of hand function over time through various compensatory pathways [3]–[7]. To enhance recovery, several interventions such as stem cell treatment, physical therapies, or electrostimulation are available. These methods have been tested in nonhuman primate models before human trials [8], [9]. Similar to humans, nonhuman primates have shown improvement through physical rehabilitation with repetitive behavioral tasks [10], [11].

Various behavioral tasks have been created to encourage the use of precision grip, the most common being derivatives of the Kluver or Brinkman board [7], [12]–[15]. The loss precision grip is, a fine movement involving coordination between the thumb and opposed fingertips to grasp an object [16], one common motor impairment in both human and nonhuman SCI populations. The Brinkman board task, a standard behavioral task commonly used with the nonhuman primate model, dates back to 1935 with the creation of the Kluver board (Figure 1.1.I) in which food rewards were hidden underneath a brass slot. The animal was expected to use one hand to lift and remove the enclosure and use the other hand to retrieve the food reward [17].

The task encouraged the use of both limbs when completing a reaching movement but did not encourage the use of the precision grip. This limitation was addressed in later Brinkman board designs (Figure 1.1.II) which required the use of precision grip to obtain the food rewards within

the wells [12]. This ideally encourages behaviors and movements similar to humans, as described in seminal works by Jeannerod and Santello which showed important findings regarding coordination between the index and thumb digits, known was preshaping [18]–[21]. Their most important finding was the temporal relationship between maximum distance between the index and thumb digits (aperture) occurs after maximum velocity in unimpaired humans [18], [19]**.** Through task design, only the impaired limb can be used to retrieve the food reward. Current implementations of the Brinkman board are heavily influenced from this design, with standard contemporary

boards shown in Figure 1.1.III [22], [23].

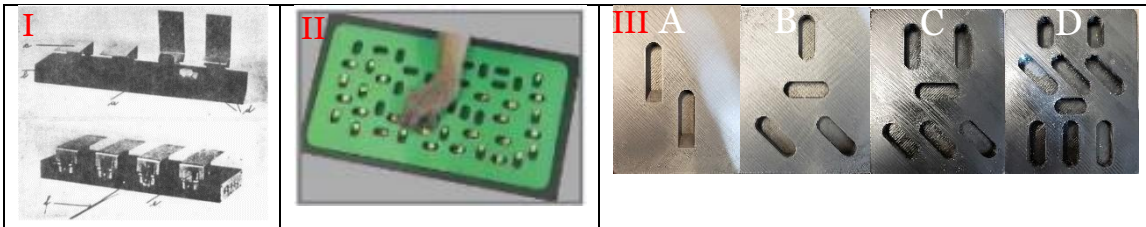

Figure 1.1. Overview of various Brinkman boards over time. (I) Origins of the Brinkman board from the Kluver board, which contains four wells each covered by a brass square. **(II)** Brinkman board that contains 50 slots (25 vertical and 25 horizontal) which encourages the use of the precision grip while the animal is in the primate chair [22]. **(III)** Cage-mounted Standard Brinkman board A-D with various numbers of slots to encourage to use of the precision grip. With the specially designed Brinkman box (Figure 1.2), these allow for home cage testing [7].

The Standard Brinkman boards (Figure 1.1.III) are designed to be used with a specially-designed cage mounted apparatus to allow animal testing in the home cage [7]. Similar to their predecessors, these boards have a variety of wells that have different well numbers, edge configurations (straight vs sloped), and orientations. Thus, animals complete several different Standard Brinkman boards to complete multiple reaching movements within one testing session.

Figure 1.2 shows an animal using the Brinkman box; their unimpaired limb pushes a lever connected to a trap door which allows the animals to interact with a Standard Brinkman board

with only their impaired limb. The animals are then scored based upon their food retrieval and use of

the precision grip on each Brinkman board. The scoring metrics are described below in Table 1.1 [7].

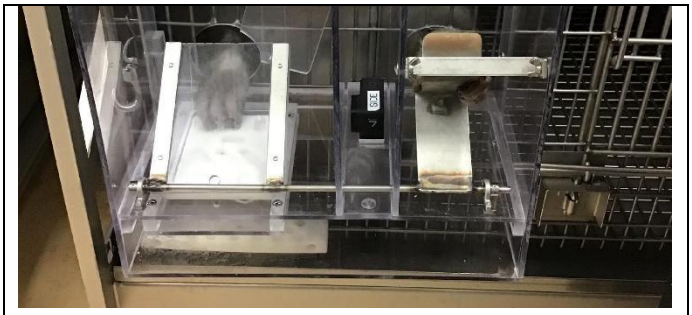

Figure 1.2. Brinkman box. Animal performing the Brinkman board task using the behavioral setup. The lever must be pushed by the left hand in order for the right hand to access the Brinkman board.

In discussion with animal trainers, they have observed that animals with more severe impairments due to their SCI, have difficulties and, sometimes stop when completing the Standard Brinkman boards. This could be due to the perception that even the simplest task too difficult, especially when previously they were able to complete the task. These difficulties are described in Darian-Smith's works where he describes the animals' inability to have coordinated reaching movements [24], [25].

Table 1.1. Scoring methodology of Brinkman board task

Scoring	**Description**
Ch (Cheated)	Animal cheated. Animal used unimpaired limb to retrieve food reward.
0 (No response)	Animal did not attempt to retrieve food reward.
1 (Attempt)	Animal reaches for and/or contacts food reward.
2 (Pick up and drop)	Animal lifts item food reward off the Brinkman board. The food reward is dropped between pick up and transfer to mouth. The animal can pick the reward up again with either impaired or nonimpaired hand to transfer to their mouth.
3 (Transfer to mouth)	Animal lifts food reward and successfully transfers to mouth or to unimpaired hand and then to mouth.
3 PNC	(Transfer to mouth with precision grip) Animal retrieves food reward using a precision grip with an impaired limb to mouth or unimpaired hand and then to mouth successfully.

Thus, there is a gap that makes it difficult to assess the animals' abilities especially early after injury, and may, reflect a learned helplessness that comes from consistent failure to complete even the simplest of the Standard Brinkman boards. This results in low scores on the behavioral assessment that do not reflect the animal's true motor ability. The current Standard Brinkman board array may be improved by creating options for success, such as expanding the size of wells to allow for a more gross movement to be successful. Inclusion of additional, Remedial Brinkman boards with larger wells could provide more opportunities for the animal to participate in the task, and lead to a score more reflective of their ability. These potential Brinkman boards would provide a remedial experience compared to the Standard Brinkman boards.

In this study, several different iterations of Brinkman boards, called Remedial Brinkman boards, were created with wells of varying sizes (20 mm, 40mm and 80 mm in width), directionality, and texture. To test whether these newer Brinkman boards provide a remedial effect, two attributes must be true: 1) The Remedial Brinkman boards must be easier to complete compared to the Standard Brinkman boards; and 2) their inclusion must positively affect performance (score increase and time of complete decrease) when completing the Standard Brinkman boards. This chapter will focus on the protocol and the associated positive motivational effects of the Remedial Brinkman boards. Commentary about the difficulty of the Remedial Brinkman boards is included in the appendix.

Protocol

1. Testing Preparation
    a. Prepare both the Standard and Remedial Brinkman boards by placing food rewards inside the wells.
    b. Place the Brinkman box apparatus on the animal's home cage.
    c. Close the port holes to disallow animal access to the Brinkman box.
    d. On laminated index card write the following:

i. Animal Name
ii. Animal ID
iii. Testing Date

2. Data Collection Set Up
    a. Place both digital cameras in their respective locations.
        i. One camera in the camera box above the testing.
        ii. One camera in the camera mount to the right (from the experimenter's point of view) of the testing area.
    b. Turn on both digital cameras with the remote
    c. Set up Brinkman board testing application with the appropriate data.
    d. Set stopwatch to 0.0 seconds.
3. Brinkman Board Testing
    a. Start recording of the testing area with the remote.
    b. Insert the laminated index card with the correct information for the animal being tested. Show the laminated index card to both the side and top cameras for approximately 3 seconds.
    c. Remove the laminated index card.
    d. Insert the Brinkman board in the Brinkman board tray within the Brinkman box.
    e. Open the port holes to allow access to the Brinkman board and start the stopwatch.
    f. The animal has 60 seconds to retrieve all the food rewards on a given Brinkman board. Their unimpaired hand must depress the lever to have

access to the Brinkman box and food rewards must be retrieved from the wells using their impaired hand.

g. Score the animal for each well appropriately as described in Table 1.1 in the introduction. Record in the Brinkman board testing application. Record the additional information below.

    i. **Proportion Precision Grip Usage** relates to how often the animal uses precision grip to pick up items:

        1. **0%**, the animal did not use the precision grip
        2. **1-49%** < 50% of the wells
        3. **50-99%** of the wells
        4. 100%, used pincer to pick up all food rewards

    ii. **Reach** relates to the animal's engagement with the task.

        1. **None**, the animal did not engage in the task or was unable to lift their arm.
        2. **Lift Arm,** the animal attempted to engage and was able to lift their arm or elbow, but not high enough to touch the port hole.
        3. **Port Hole**, the animal was able to reach the port hole but not touch the Brinkman board.
        4. **Touch Board**, the animal was able to touch the board.

    iii. **Cheat** indicates whether the animal successfully cheated. Cheating is defined as using the unimpaired hand to retrieve the food reinforcers from the well. If the animal cheated, they receive a score of 0.

1. **No**, the animal did not cheat.
2. **Yes**, the animal successfully cheated.

h. Stop the stopwatch once the animal has retrieved all food rewards or once the animal reaches the 60 second timeout. Then using the remote, stop recording. Record their time in the Brinkman board application.

i. Remove the completed Brinkman board from the Brinkman board tray.

j. Close the port hole.

k. Insert the next Brinkman board.

l. Repeat steps a-k for the remaining Brinkman boards in Figure 1.3.

4. Standardized Brinkman board order.

a. Figure 1.3 is the standardized order to administer the Standard and Remedial Brinkman boards. Brinkman boards outlined in a red box are the Remedial Brinkman boards. Figure 1.3A is designated a Level 1 Remedial Brinkman board with the largest well

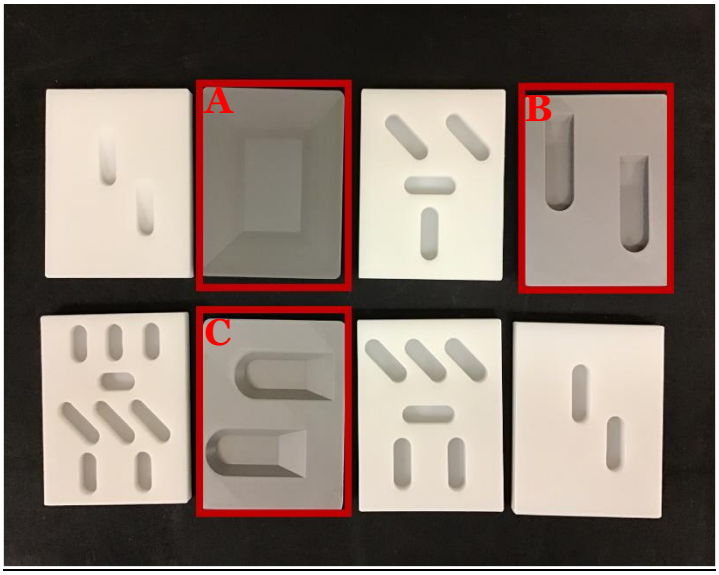

Figure 1.3. Remedial Brinkman boards (grey) incorporated into the Standard Brinkman board (white) task in a standardized order. Three Remedial Brinkman board designs were chosen **(A-C)**. **(A)** Example of a Level 1 Remedial Brinkman board due to its large well size. **(B)** Example of a two-sloped, vertically oriented Remedial Brinkman board with a well size of 20mm in width. **(C)** Example of a horizontally oriented Remedial Brinkman board with sloped edges and a well size of 20mm in width. Both B and C are categorized as Level 2 Remedial Brinkman boards.

size of 40mm or 80 mm. Figure 1.3B and Figure 1.3C are Level 2 Remedial Brinkman boards with a well size of 20mm and differ in orientation.

b. Level 1 and Level 2 Remedial Brinkman boards can be substituted with any other Brinkman board within the same level as show in Figure 1.4 as long as the animal receives: one Level 1 Remedial Brinkman board, one Level 2 Vertical Remedial Brinkman board and one Level 2 Horizontal Remedial Brinkman board.

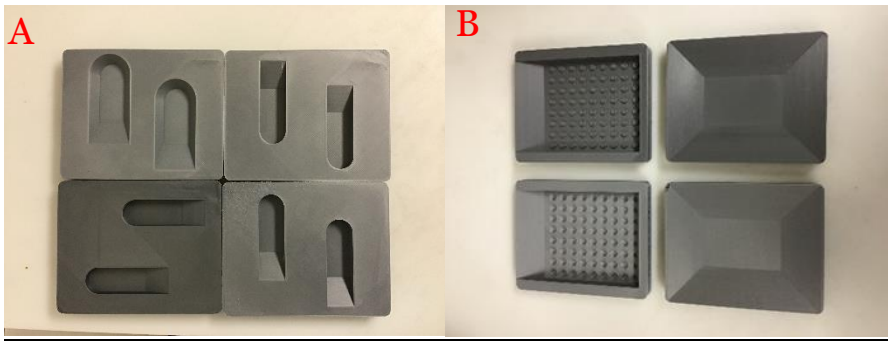

Figure 1.4. Sample of Remedial Brinkman boards. (A) Remedial Brinkman boards Level 2. These boards have a width of 20 mm. Directionality and number of sloped edges may vary. **(B)** Remedial Brinkman boards Level 1. These are any boards with a well size larger than 40mm. They can contain physical features such as a Lego surface or four slopes.

5. Clean up
    a. After completion of all Brinkman boards, soak the Brinkman boards in warm tap water with a cleaning agent.
    b. Scrub off any remaining residue with a rag or sponge.
    c. Inspect the Brinkman boards for damage, specifically on the testing surface or within the wells. Replace any Brinkman boards with significant damage such as a hole. Cleaning agents could be trapped inside it which can be potentially dangerous to the animal.

Animal characteristics

In this study, two male rhesus macaques (*Macaca mulatta,* age: 6 years, 6 months; weight: 12.1 kg and age: 7 years, 6 months; weight 14.6 kg) were used. The Remedial Brinkman boards were introduced late into their recovery after a hemisection lesion to the spinal cord at C5- C6 and after treatment. The nature of their treatment was blinded to the experimenter.

All animals in the study were housed at the California National Primate Research Center, Davis, CA; all primate procedures were approved by the California National Primate Research Center Institutional Animal Care and Use Committee

Summarized Results

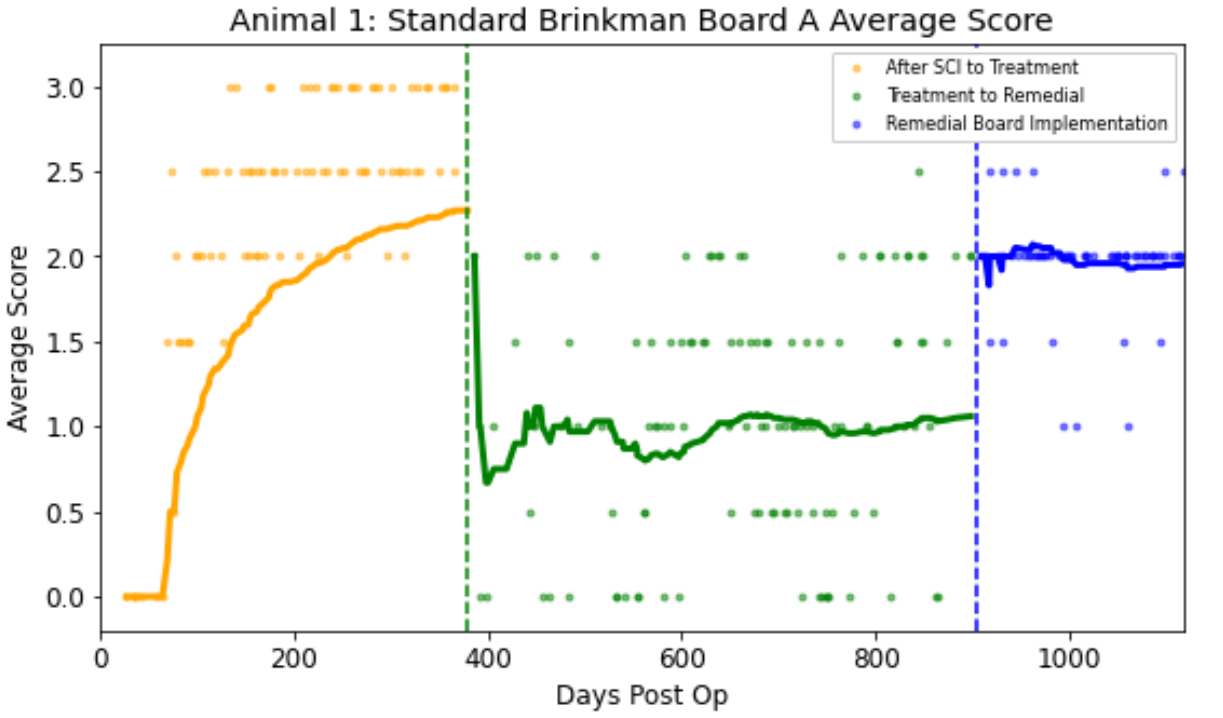

Figure 1.5. Animal 1 Standard Brinkman board A score. The three different colors represent three different time periods (yellow: After SCI to Treatment; green: Treatment to Remedial; blue: Remedial Board Implementation). The individual dots represent the average score on a given day. The rolling average for each section was calculated and represented by the solid line in their respective colors.

The final average scores on Standard Brinkman board A (Figure 1.1.III.A) for the three time periods ("After SCI to Treatment", "Treatment to Remedial", and "Remedial Board Implementation" were 2.27, 1.09, and 1.96. A causal impact analysis was conducted between the "Treatment to Remedial" and the "Remedial Board Implementation" sections to determine the effect of the Remedial Brinkman boards. The Remedial Brinkman boards were shown to have a significant positive effect (probability <0.05) on board A.

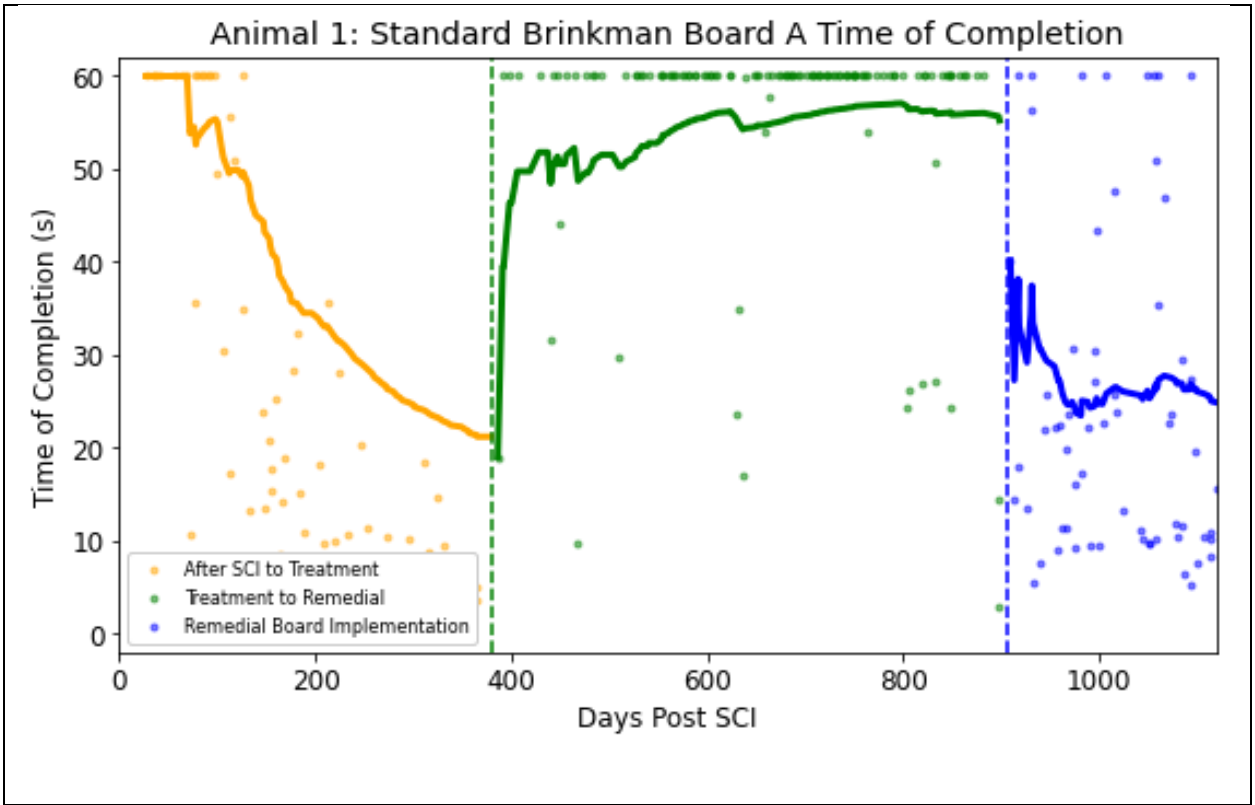

Figure 1.6. Animal 1 Standard Brinkman board A time of completion. The three different colors represent three different time periods (yellow: After SCI to Treatment; green: Treatment to Remedial; blue: Remedial Board Implementation). The individual dots represent the time of completion on a given day. The rolling average for each section was calculated and represented by the line in their respective colors.

The final average completion time scores for the three time periods (“After SCI to Treatment”, “Treatment to Remedial”, and “Remedial Board Implementation”) were 21.2 seconds, 55.23 seconds, and 24.89 seconds. A causal impact analysis was conducted between the “Treatment to Remedial” and the “Remedial Board Implementation” sections to determine the effect of the Remedial Brinkman boards and were shown to have a significant positive effect (probability<0.05) in this animal.

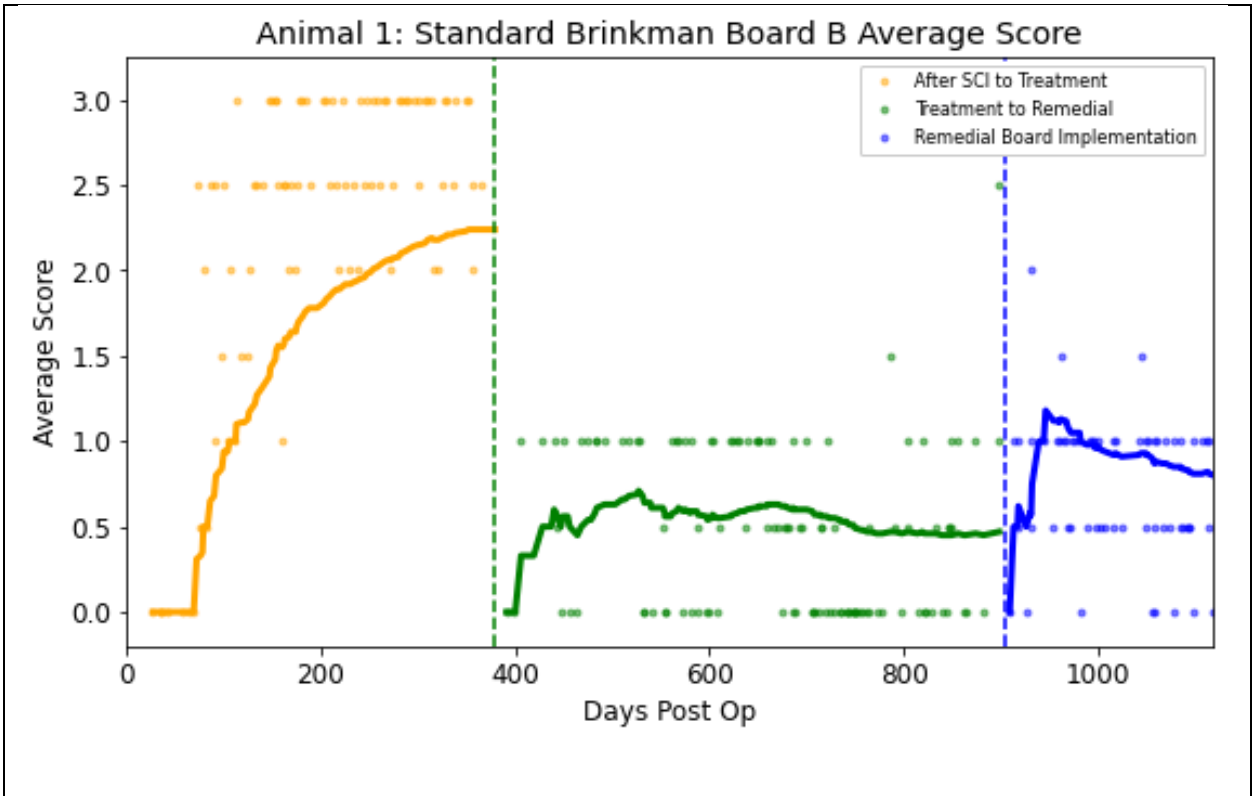

Figure 1.7. Animal 1 Standard Brinkman board B score. The three different colors represent three different time periods (yellow: After SCI to Treatment; green: Treatment to Remedial; blue: Remedial Board Implementation). The individual dots represent the average score on a given day. The rolling average for each section was calculated and represented by the line in their respective colors.

The final average scores on Standard Brinkman board B for the three time periods were 2.24, 0.47, and 0.80. A causal impact analysis was conducted between the “Treatment to Remedial”

and the “Remedial Board Implementation” sections to determine the effectiveness of the Remedial Brinkman boards and were shown to have a significant positive effect (probability<0.05) on performance in this animal.

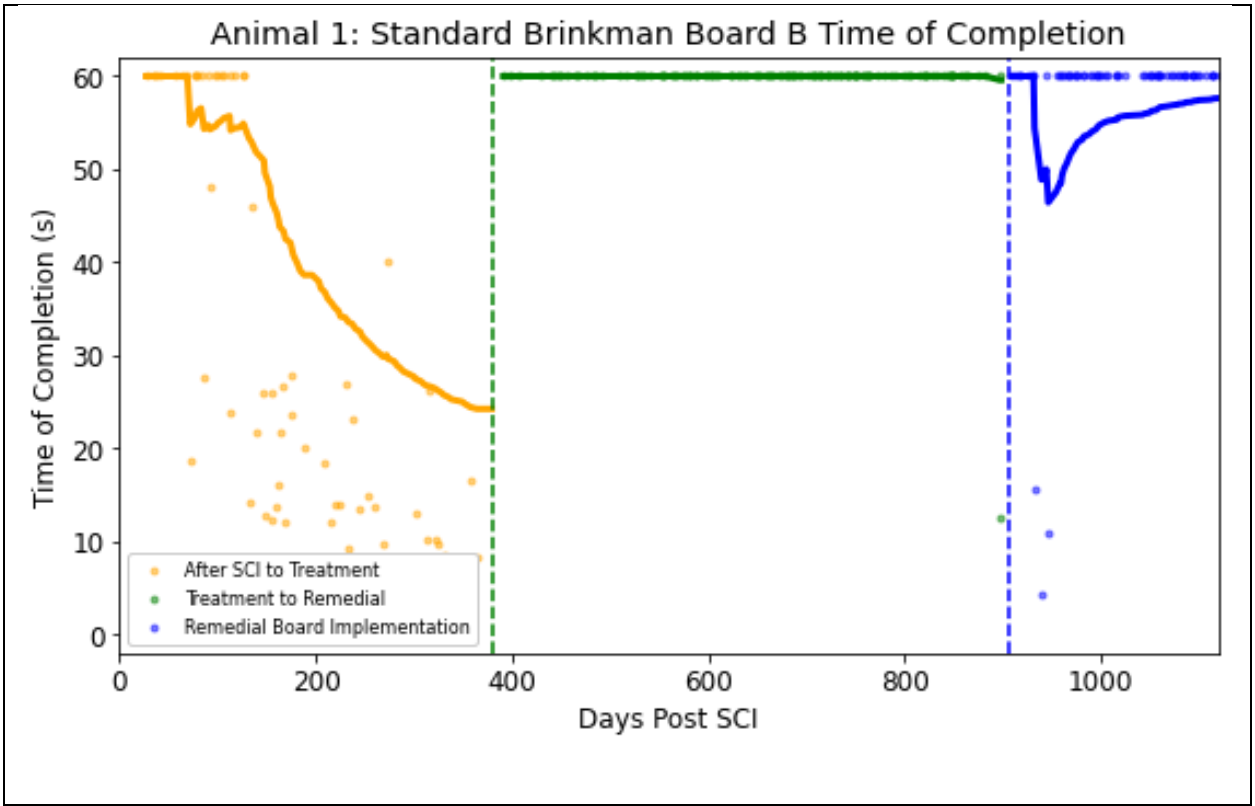

Figure 1.8. Animal 1 Standard Brinkman board B time of completion. The three different colors represent three different time periods (yellow: After SCI to Treatment; green: Treatment to Remedial; blue: Remedial Board Implementation). The individual dots represent the time of completion on a given day. The rolling average for each section was calculated and represented by the line in their respective colors.

The final average completion time scores for the three time periods were 24.25 seconds, 60 seconds, and 57.63 seconds. A causal impact analysis was conducted between the “Treatment to Remedial” and the “Remedial Board Implementation” sections to determine the effectiveness of the Remedial Brinkman boards. The Remedial Brinkman boards were shown to have no effect, on the completions times for this animal.

Animal 1 Count Data Results

Count data were collected based on Animal 1's performance using Standard Brinkman board A and B. From Table 1.1, a score of 0 represents no attempt. The total number of 0 scores were tallied and a percentage of 0 scores was calculated based upon the time period in which they occurred. Similarly, the number of times animal 1 had a 60 second timeout (i.e. did not clear the Standard Brinkman boards A or B in the allotted time or did not participate) was also tallied. The percentage of timeouts was calculated based on the time period in which they occurred.

Table 1.2. Animal 1 Standard Brinkman board A 0 Score Counter.

Time Frame	0 Score Trials	Total Trials	Percentage of 0 score
After SCI to Treatment	6	88	6.82
Treatment to Remedial	22	119	18.49
Remedial Board Implementation	0	63	0

Table 1.3. Animal 1 Standard Brinkman board A 60 Second Time of Completion Counter.

Time Frame	60 Second Trials	Total Trials	Percentage of 60 Trials
After SCI to treatment	15	88	17.05
Treatment to Remedial	99	119	83.19
Remedial Board Implementation	8	63	12.7

Table 1.4. Animal 1 Standard Brinkman board B 0 score counter.

Time Frame	0 Score Trials	Total Trials	Percentage of 0 score
After SCI to Treatment	7	87	8.05
Treatment to Remedial	51	115	44.35
Remedial Board Implementation	8	63	12.7

Table 1.5. Animal 1 Standard Brinkman board B 60 Second Time of Completion Counter.			
Time Frame	60 Second Trials	Total Trials	Percentage of 60 Trials
Before Treatment	20	87	22.99
Treatment to Remedial	114	115	99.13
Remedial Board Implementation	60	63	95.24

From this data, a proportional z test was conducted. The z statistic and resulting p values are tabulated in Table 1.6 below. All metrics except Standard Brinkman board B time of completion were determined to be significant. The results of all the proportional z test are similar to the results of the causal impact analysis. These results suggest that the implementation of the Remedial Brinkman boards had an overall positive effect on performance on Standard Brinkman boards A and B for this animal.

Table 1.6. Animal 1 Proportional Z test Results between Treatment to Remedial and Remedial Board Implementation Sections.		
Board	Z- Statistic	P value
Standard Brinkman board A Score	3.64	P<0.001
Standard Brinkman board B Score	4.29	P<0.001
Standard Brinkman board A Time of completion	9.19	P<0.001
Standard Brinkman board B Time of completion	1.68	P=0.05

Discussion

Animal 1's average score on Standard Brinkman board A is interesting in that his performance in the "After SCI to Treatment" time period showed some recovery (2.27 points out of 3 possible) but then demonstrated a decrease in performance "After Treatment" (1.09). This suggests that Animal 1, on average, was completing the Standard Brinkman boards and then stopped regularly

completing it after treatment. This behavior is mirrored in Figure 1.6 showing the average time of completion decreased in the "After SCI to Treatment" section (21.2 seconds) but then had a high average time of completion in the "Treatment to Remedial" section (55.23). In the "Remedial Board Implementation" section, a jump in average score (from 1.09 to 1.96) occurred and achieved relative stability. The time of completion data reflected this pattern as well (from 55.23 to 24.89 seconds). From the interrupted timeseries analysis, it is highly unlikely that these results occurred by chance (score: probability < 0.001; time of completion: probability < 0.001).

Upon closer inspection, this is partially a result from a 0 score and 60 second percentage decrease as shown in Tables 1.2 and 1.3. These decreased percentages (Treatment to Remedial vs Remedial Board Implementation) were significant ($p<0.001$, Proportional Z-Test). These improvements suggest Animal 1 was capable of completing the sloped two well task (board A), and on average retrieved the food reward in each well. Performance on Board B (non-sloped two well task) proved more difficult. After remedial board implementation, a jump in average score (from 0.47 to 0.80) occurred ($p<0.05$), but the time of completion data did not change significantly (from 60 to 57.63 seconds; not significant). Thus, the remedial boards improved performance on the easiest standard boards.

This result is in line with other positive reinforcement training research [26]–[30]. The animal is receiving more opportunities to participate in tasks with Remedial Brinkman boards. Another notable point is that participation in this task is voluntary. The animal could easily be presented the task and choose not to participate if there's little interest, or if the task is too difficult [31]; this did result in the 0 scores and 60 second "timeouts", specifically in the After SCI to Treatment section.

In terms of Standard Brinkman board B, Animal 1's performance also shows improvement after Remedial Brinkman board implementation (0.47 vs .80 score and 60 seconds vs 57.63 seconds) but does not reach the same level of performance before treatment was administered (2.24 and

24.25 seconds). Table 1.4 shows that the percentage of 0 scores does decrease. This suggests that the animal was engaging with the task, but was not necessarily successful; additionally, the animal was receiving a score of 1 and not 0 which would increase the average score.

In the 60 second counter percentage, the animal continued to "timeout" at 60 seconds, which further suggests that the animal was participating but not successfully completing the task. The animal also attempted to use a raking motion [32], a claw-like action where they placed the tips of their digits on the top of the Brinkman boards and dragged the food reinforcer out. Despite these smaller improvements, the Remedial Brinkman boards do provide significant increases in interaction with the task and improvement in performance.

Limitations

Incorporating additional, Remedial Brinkman boards in the behavioral testing protocol presents unique challenges in its implementation. These can be broken down into two main categories: animal health and manufacturing challenges.

As previously mentioned, animals after spinal cord injury have difficulties when completing dexterous hand movements. This may cause the animal to overexert themselves when completing the Brinkman board task, which can lead to the incompletion of the remaining Brinkman boards. While this behavior typically occurs earlier in the recovery period post SCI operation, it has not been an issue when consulting with primate experts. This may differ with other animal models but remains untested.

In terms of manufacturing, the Remedial Brinkman boards are currently 3D printed using ABS plastic. While this does pose a number of advantages such as low-cost printing and rapid prototyping for new Brinkman boards, the printing material could be an issue. Over time, the plastic of the boards can deteriorate, specifically the corners and back side. This damage is

superficial and does not impact the function of the Remedial Brinkman boards. Examples of the damage can be seen in Figure 1.9 below.

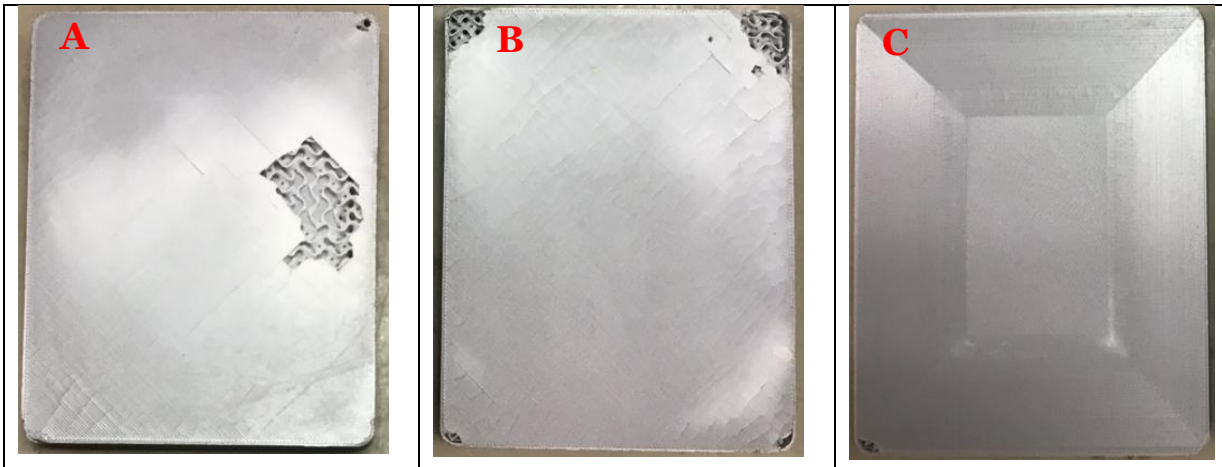

Figure 1.9. Deterioration of Remedial Brinkman board using ABS plastic. The plastic surface deteriorates, showing the hexagonal infill shaping. This shaping provides the structural support for the Remedial Brinkman board and conserves material. This also has the added benefit of reducing manufacturing time of each Brinkman board. **(A)** Damage near the center on the backside of the Remedial Brinkman board. **(B)** Damage on each corner on the backside of the Remedial Brinkman board. **(C)** Damage in the corner of the top surface of a Remedial Brinkman board. Surface damage as seen on this Remedial Brinkman board can cause some concern as the animal could potentially scrape off the material and consume it, even if non-toxic. This type of damage was rare and was only seen on one of the 35 Remedial Brinkman boards constructed.

Current anecdotal evidence and the cleaning procedures place an effective 18-month lifespan for a Remedial Brinkman board. Boards were replaced before there was visual damage to the top surface where the food rewards are placed. The effective lifespan could be improved by adding more infill material or by replacing the ABS plastic with another material. Using a different material may require using a different manufacturing technique but could also increase the lifespan of the Remedial Brinkman boards.

Conclusion

The Brinkman board task is a reach and grasp activity designed to facilitate the use of precision grip in the nonhuman primate model. After spinal cord injury, this type of behavior is challenging for the animals to complete and can be used as an assessment tool for recovery and treatment effects. Without proper motivation, the animals can become discouraged and not participate in the Brinkman board task. This would suggest that recovery has stopped, which could be incorrect. This specific behavior is seen with Animal 1. The Remedial Brinkman boards provide additional opportunities for the animals to retrieve food rewards with a lower difficulty. These additional opportunities then manifest in an increase in the animals' participation and performance, which are more indicative of their true recovery potential.

Chapter 2: Create and apply the use of the modified apparatus with the use of a neural network for kinematic analysis

Summary Statement

DeepLabCut can be used to track and quantify fine movement of individual digits in nonhuman primates, facilitating the kinematic analysis of reaching and grasping without physical markers.

Abstract

The ability to assess reaching and grasping patterns is of particular interest in clinical conditions that affect the motor system (e.g., spinal cord injury (SCI)) but is frequently limited to behavioral observational techniques to assess functional recovery.

Here, the use of DeepLabCut, an open-source deep learning toolset, in combination with a standard behavioral task to quantify nonhuman primate performance in precision grasping, was examined. Two neural networks were trained on 450 paired video frames to track 19 unique landmarks of one rhesus macaque completing the standard behavioral task. Based on previous reports, this neural network produced sufficient tracking, with test pixel errors of 11.25 (max error of 1.04%) and 30.31 (max error of 2.81%) pixels. Additionally, using DeepLabCut over previous post-hoc manual annotation methods has significant time savings and affords an economy of scale. These results suggest that DeepLabCut is an effective method to examine kinematic features of hand function in animal models of motor impairment in the non-human primate model.

Introduction

Behavioral assessments of motor function in animal models of disease have ranged from observational rating scales (e.g., Basso, Beattie, Bresnahan, BBB Locomotor Rating Scale [31]), to simple measures on set tasks (e.g., time required for reward retrievals [32], [33]) to 3D kinematic metrics requiring advanced equipment and analytical techniques [34], [35]. Similarly, for human clinical assessment, scales such as the Jebsen-Taylor Hand function test or the GRASSP test have been used to evaluate activities of daily living for patients [36]–[38]. These include, but are not limited to, patients' strength, prehension ability, and prehension performance graded on a 0 to 4 scale. In the nonhuman primate model, the Modified Non-Human Primate Grasp Assessment Scale created by Moore et al. in 2012 has been adopted and updated over the last several years to include more levels for increased sensitivity [39]–[41]. The first version of the Modified Non-Human Primate Grasp Assessment Scale was based on the Fugl-Meyer Motor assessment scale and the Eshkol-Washman Movement Notation [39], [42], [43]. While scales are powerful benchmarking tools and provide standardization across experiments and studies, they do not provide quantitative measures of movement kinematics (e.g., changes in position or velocity).

To obtain kinematic information, one common approach is to place physical markers at specific anatomical locations on animals to focus on joint movement. For example, Courtine et al. used reflective markers at bony landmarks in rats to obtain the walking pattern of the animals before and after injury [34]. In nonhuman primates, physical markers in conjunction with motion capture systems have been used to quantitatively examine reaching and grasping behavior [35], [44]. Other studies have used reflective paint on landmarks in conjunction with motion capture systems [45]–[48]. This type of quantitative data collection has provided more information on detailed motor behavior while concurrently obtaining simpler measures of task performance such as success rate, time to completion, etc. However, these types of marker-based tracking methods can affect the natural behavior of the animal, and subsequently affect behavioral analysis [49],

[50]. For example, the animal can become distracted by the physical marker and attempt to take it off. To avoid affecting the natural behavior of the animal, manual annotation of videos post-hoc has been used, such as the ones used by Pizzimenti [51]. This process is time consuming and increases exponentially with the number of frames recorded.

Recently, more advanced computational techniques such as DeepLabCut allow for the tracking of anatomical locations without the use of physical markers during movement [52]. Previous uses of DeepLabCut include reach and grasp tasks for mice (3D information) and more naturalistic studies conducted on nonhuman primates (2D information) [44], [52]–[56]. In both animal models, DeepLabCut was able to achieve sufficient tracking so that further quantitative analysis could be performed through accurately tracked specific landmarks (e.g., the individual digits in the rat model) allowing further analyses of movement kinematics.

Presented here is a methodology which allows for the recording and analysis of behavioral data when using DeepLabCut in the non-human primate model [57], [58]. This study demonstrates the feasibility of tracking specific landmarks which relate to anatomical features on the digits, without the use of physical markers, for kinematic analysis. This is an advancement over previous techniques since natural grasping behavior is minimally influenced and there is the potential for significant time savings compared to manual annotation.

Methods

Animals

In this study, two rhesus macaques (*Maca mulatta*, male, 7 years, 11 months, weight 11.70 kg and female 10 years, 5 months, 10.06k) were used. These animals were housed at the California National Primate Research Center, Davis, CA; all primate procedures were approved by the California National Primate Research Center Institutional Animal Care and Use Committee.

Behavioral Hand Task (The Brinkman Board Task) for Nonhuman Primates

Each animal was trained to use their right hand to retrieve food rewards from the wells on a Standard Brinkman board using the precision grip, which is the dexterous use of the index and thumb digits to grasp an item. An idealized version of this grip in the context of the Brinkman board is shown in Figure 2.1. These rewards were varied to optimize the animal's motivation (e.g. yogurt covered raisins, nuts, etc.) but maintained a consistent reward size. Performance on the board was assessed by a numerical score (between 0-3) based on the animal's ability to retrieve food rewards without dropping them, and transfer that reward to their mouth. In this study, all retrievals were scored a 3, which indicates that the animal successfully retrieved the food reward without dropping it.

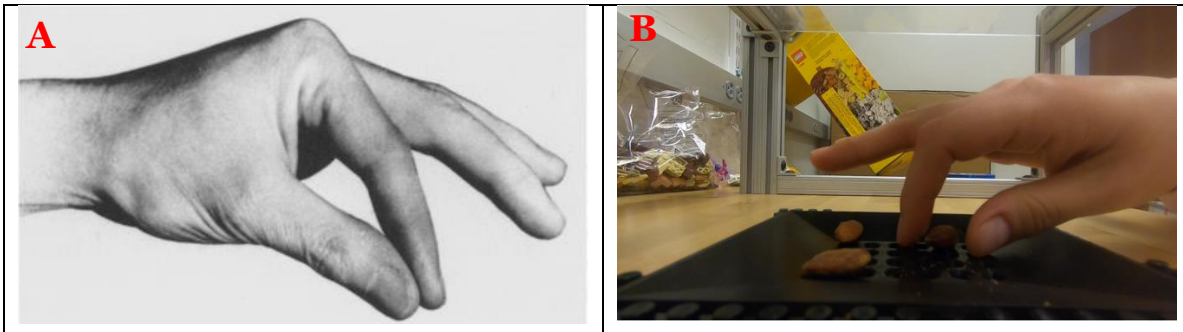

Figure 2.1. Precision grip. **(A)** The ideal precision grip depicted by Napier [14]. An object would be squeezed and controlled using the pads of the index and thumb digits. **(B)** Mid-recording screenshot of the precision grip during the Brinkman board task. The index and thumb digits are approaching the almond between them. This an example of the precision grip used in the context of the Brinkman board task.

Each animal was given 60 seconds to retrieve all the food rewards from each board. In the analysis described here, eight unique Brinkman boards were presented, which constituted one session. Each animal then completed two more sessions on the same day to allow for more videos to be included in the DeepLabCut training. These Brinkman boards varied in the number of wells (1-9) and the well orientation are shown in Figure 2.2.

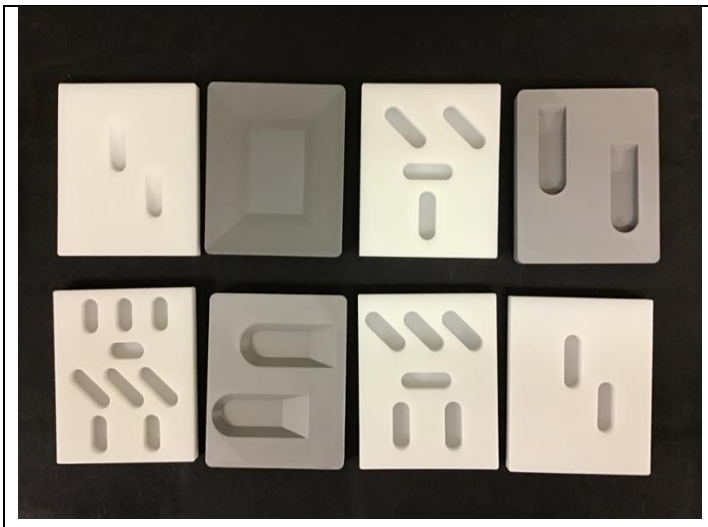

Figure 2.2. Depiction of example Brinkman boards. Note the differences in the number of reward wells (1, 2, 4, 7 and 9), orientation, and size with respect to hand movement (45°,90°, and 180°).

Video Collection

Two small identical digital cameras (GoPro Hero7 Black, GoPro, San Mateo, California, United States of America) were used to record animals while they completed the Brinkman board task. The apparatus was modified to include the cameras, one camera was placed above and another to the side of the testing area as shown in Figures 2.3A and 2.3B below. Each camera is outlined in the red box. Both cameras were not accessible to the animal. Recording started when the Brinkman board was accessible to the animal and ended when the animal completed the session. The recordings were complete at a resolution of 1920 by 1080 pixel and a frame rate of 120 frames per second.

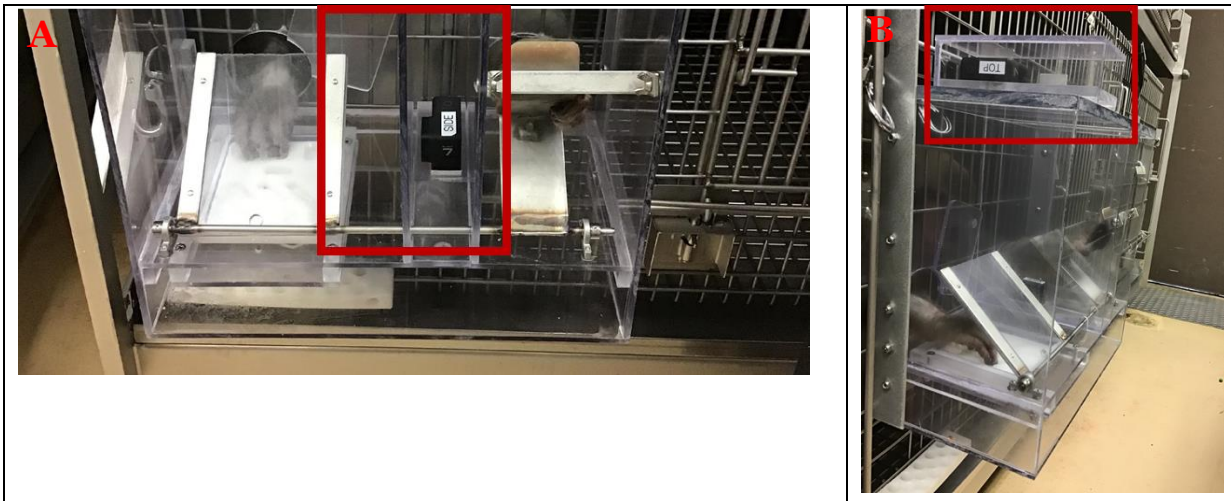

Figure 2.3 Front view of Camera Supporting Brinkman Box in use. (A) The animal's left hand is being used to depress the lever that allows for the Brinkman board to be accessible to the right hand. Outlined in the red box is the side view camera, inaccessible to the animal. Furthermore, the animal is not distracted by the presence of the camera. **(B)** Isometric view of Camera Supporting Brinkman Box in use. The animal's right hand is shown interacting with the Brinkman board. Outlined in the red box is the top view camera. A small housing was created to encapsulate the camera to ensure the animal could not access the camera. Discussion of the development of this apparatus is included in the appendix.

Data Generation

Fourteen features of interest consisting of each knuckle and fingertip were manually annotated to be tracked by two separate DeepLabCut neural networks (top and side views). These locations are tabulated below (Table 2.1). Four hundred paired frames were manually annotated for DeepLabCut training. A guide to replicate the steps taken to train these neural networks is included in the appendix. This guide is based upon Mathis et al. paper [52] that serves as a walkthrough for DeepLabCut.

Table 2.1. Features of interest for nonhuman primate tracking.

Feature	Locations
Thumb Digit (D1)	Fingertip and 1st Knuckle
Index Digit (D2)	Fingertip, 1st Knuckle, and 2nd Knuckle
Middle Digit (D3)	Fingertip, 1st Knuckle, and 2nd Knuckle,
Ring Digit (D4)	Fingertip, 1st Knuckle, and 2nd Knuckle
Pinky Digit (D5)	Fingertip, 1st Knuckle, and 2nd Knuckle

Results

Network Training

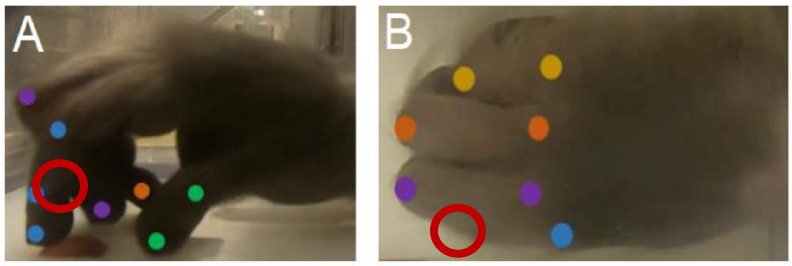

Figure 2.4. Automatic tracking on the nonhuman primate hand during the Brinkman board task. (A) Side view of marked locations. Only the index and thumb digits are fully markered. The remaining locations are occluded from this camera angle. For example, the 1st knuckle of the middle digit (D3) is occluded by the index digit (D2) (red circle). **(B)** Top view of markered locations at a different timepoint with respect to panel A. The top view mainly focuses on the 2nd and 3rd knuckle locations of all the digits. Similar to panel A, not all locations are markered as they are occluded by other digits. Specifically, the 2nd knuckle of the index digit (D2) is folded under (occluded) the middle digit (D3) (red circle).

Two networks were trained corresponding to the two cameras (top and side) using 400 manually annotated images from 16 different videos (25 images from each video determined by a k-means algorithm for visual uniqueness) from two separate sessions of the Brinkman board task. In these annotated images, the locations of the fingertips and knuckles of the five digits in the right hand were of interest in the videos as summarized in Table 2.1. Examples of the side and top view camera frames, with the color-coded markers of the landmarks, are shown in Figure 2.4A and B, respectively. Lastly, the performance on all videos obtained during the Brinkman board task used in the network trainings were scored as 3, the highest score possible in which the animal retrieves the food reward without dropping it.

Following the recommended procedure and the methodology described in the appendix, this method yielded a side camera trained pixel error of 2.15 (this represents the root mean square error between user and DeepLabCut values using images the DeepLabCut neural network was trained on), and a test pixel error of 11.25 (which represents a max error of 1.04%; this error is the root mean square error between the user and DeepLabCut using images naïve to the DeepLabCut

neural network training). For the top camera the trained pixel error was 2.06, and the test pixel error was 30.31 (max error of 2.81%). Using the linear conversion from pixel to cm, this translates to a maximum error of 0.1 cm. These values were comparable to a previous primate study, and were judged sufficient for additional tracking on the remaining videos [59]. This procedure outputs a .csv file similar to other kinematic tracking systems such as the location and a confidence value for a given tracked location at each timepoint.

Time Investment

Below is Table 2.2 consisting of the time investment for training and using one DeepLabCut neural network. Each step is a part of the analysis sequence outlined in the step-by-step guide included in the appendix. The table is broken down into two major sections, for each network and for each

Table 2.2. Estimated time requirement to fully train the DeepLabCut neural network for non-human primate use. The steps are broken down into two sections, for each network and for each video. After a network has been trained and is evaluated for accuracy, there is no additional time investment into the network. The remaining time investment is in automatic video annotation.

	Step	Time Required (Hours)
For each network	Step 1: Video Import	4
	Step 2: Video Conversion	2
	Step 3: Start DeepLabCut File	1/3
	Step 4: Import Videos into DeepLabCut	1/3
	Step 5: Extract Frames	3
	Step 6: Label Frames	16
	Step 6: Create Skeleton	1
	Step 8: Create Training Set	1
	Step 9: Train Network	9
	Step 10: Evaluate Network	1
For each video	Step 11: Track Locations	¼ per video
	Step 12: Create Annotated Videos	¼ per video
	Total time	37.6 + .5 per annotated video

video. Once a network is trained and evaluated, the process does not need to be repeated. There is a 30-minute time investment for each video annotated after a network has been trained.

Discussion

Using DeepLabCut

DeepLabCut is a deep neural network capable of learning myriad behaviors ranging from gait to the reaching behaviors seen here. Previously trained neural networks focused on the nonhuman primate model such as MacaquePose and OpenMonkeyStudio focus on full body tracking. Since these existing networks do not focus on hand kinematics, it was determined that training neural networks with a focus on reaching behaviors in the nonhuman primate model would be best. In this case, two networks were trained in a common reach and grasp task, the Brinkman board task, that is commonly used to assess nonhuman primates. The DeepLabCut networks trained here focus solely on the hand kinematics without the tracking of other locations.

Potential Time Saving

One of the largest potential limitations of using DeepLabCut is the initial time needed to track landmarks in the nonhuman primate model. Table 2.3 contains the time invested in annotating five videos compared to a manual annotation approach by Pizzimenti [51]. In Pizzimenti's study, nonhuman primates completed a hand dexterity task in which food pellets were placed in wells of a custom apparatus encouraging the use of the precision grip, similar to the Brinkman board. This custom apparatus had reflective markers placed throughout the space, which allowed for the space to be calibrated in 3D space, a significant advantage over the methodology presented here. The caveat to this system is the large time investment needed to manually annotate each frame for the presence of the nonhuman primate hand. It's estimated that it would require 44.4 hours to manually annotate five videos recorded at 100 hz assuming that only the index and thumb digit

fingertips are tracked. DeepLabCut is estimated to take 40.1 hours, approximately 4 hours in time savings. Time savings increase as the number of videos increase as shown in Table 2.3 below. This table describes how DeepLabcut affords an economy of scale over manual annotation.

Table 2.3. Time investment comparison between manual annotation approach vs DeepLabCut approach.

Number of Videos Annotated	Manual Annotation Approach (hr)	DeepLabCut (hr)
5	44.4	40.1
10	88.8	45.1
20	177.6	55.1

While this is the most direct method for comparison to post hoc labeling, other systems that include physical labelling of landmarks can produce kinematic tracking in potentially shorter times. For example, Courtine et al. used reflective paint on specific landmarks such as the knee joint in determining the gait kinematics of nonhuman primates [34]. This type of labeling system includes shaving the animal's joint locations, which can be undesirable. Another example would be to tape markers to desired locations, such as in studies by Roy et al. [60]. These types of studies can lead to performance differences that may be detrimental, but do not have the same time limitations as the manual annotation approach [49], [50]. Additionally, these markers would need to be reapplied for every recorded video which could lead to tracking variability. Other systems, such as the Plexon system, allow for automated tracking of the nonhuman primate model, but information about the time investment, associated costs, and tracking accuracy is limited [61].

Limitations

DeepLabCut has demonstrated a strong case for use in non-human primate studies. Using the built-in benchmark, DeepLabCut was able to track user defined locations to the mm level, but this benchmark does not consider frames where the hand was in frame and unable to be tracked. This can be seen in the figure below where the hand is significantly blurred. The individual locations are difficult to discern as compared to the nonblurred image. This is a byproduct of two main factors.

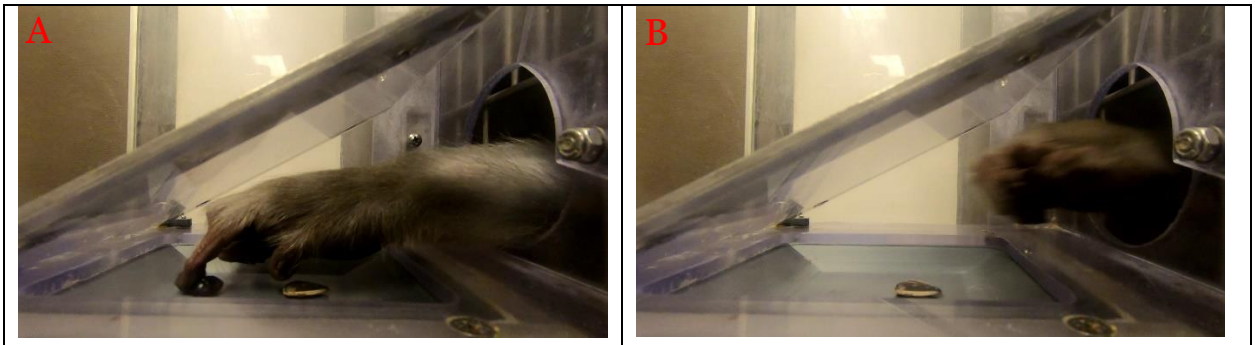

Figure 2.5. Nonhuman primate hand during the Brinkman board task. (A) Limited motion blur image of nonhuman primate hand during the Brinkman board task. The index digit is currently in contact with the food reward with the thumb digit closing in. Both digits of interest, the index and thumb digits, are clearly visible and blurring is at a minimum. This would allow for manual annotation to be relatively straightforward. **(B)** Significantly blurred image of nonhuman primate during the Brinkman board task. The hand is moving toward the animal's mouth in possession of the food reward. The individual digits are difficult to discern, and the food reward cannot be clearly seen. In motion and to the human eye, this frame would appear normal. To a neural network, the image would appear to be unique and could be a potential source of error. During the manual annotation phase, this would be difficult to annotate properly, leading to another potential source of error.

Firstly, the neural network was specifically not trained on blurred frames to increase accuracy as specified by Mathis et al [52]. If the annotator is not confident in the location within a frame, it is skipped. This is to prevent the neural network from learning a poor behavior. Thus, for the network to track these locations the blurred factor of the frame must be reduced. This can be done during recording or post-hoc with deblurring techniques such as the ones described in Mahesh et al. [62]. Techniques for reducing blurred frames during recording are discussed in the appendix.

Secondly, the nature of the hand moving out of frame might cause tracking to be limited. This theory has been postulated by other researchers in their studies with rat images [63]. In Kirkpatrick's study, DeepLabCut was trained to track landmark locations using x-ray images. In a subset of images, the desired landmark to be tracked was out of frame, leading to abnormally higher levels of variations in tracking [63]. This theory might address why the pixel error presented in this non-human primate case is higher than those predicted by Mathis et al. where the desired locations are always in frame [52].

Conclusion

DeepLabCut is a deep neural network that can automatically track desired locations after training. The use of these networks has substantially reduced the time to manually annotate frames that were later used for kinematic analysis. This type of kinematic analysis is limited by the blurred images that occur during recording. Previous work details the specific nuances implementing either a post-hoc or recording solution which could help circumvent this limitation. In combination with standard electronic recording cameras and no physical markers, DeepLabCut and similar neural network software programs offer a unique solution for movement kinematic analysis, an approach that was previously considered to be too difficult to implement without significant compromises in changing naturalistic behavior.

Chapter 3: Quantification of 2D hand kinematics of nonhuman primates using high resolution quantitative data

Summary Statement

Previous non-human primate works focus on low resolution quantitative metrics, such as discrete number scaling, to describe metrics during behavioral testing. This is specifically important when determining treatment effects and quality of recovery in the spinal cord injury model.

Outcome measures can be improved upon by including high resolution quantitative metrics using kinematic tracking. This allows for the exploration of deeper relationships such as the ones between velocity and maximum aperture during grasping. Early studies uncovered these temporal relationships in the unimpaired non-human primate model.

Using newer technologies that allow for tracking without physical markers, the timecourse of recovery for these temporal relationships were determined. These additional insights can help guide the design and implementation of future treatments.

Abstract

Non-human primate works currently focus on low resolution quantitative metrics, such as the Brinkman board task, to describe motor performance. Previous research in humans and non-humans have determined that there are temporal relationships that describe reach and grasp through kinematic analysis. Additionally, with current advances in neural network it is possible to track individual digits without physical markers. Using the methodology from Chapter 2 for determining locations of physical landmarks, this study looks to determine if these timing relationships during a reaching movement, such as the aperture-velocity timing relationship, are independent of the reach and grasp task. Two non-human primates were trained and recorded participating in a standard behavioral task, the Brinkman board task.

Over 22 reaching motions, it was determined that there is a temporal relationship between maximum aperture (distance between index digit and the thumb digit) and minimum velocity during reach and grasp. There was no temporal relationship between maximum finger extension and maximum aperture. Other previously determined relationships such as the timing of maximum aperture and maximum velocity could not be quantified because the recording window for this study is different than that of previous studies. Regardless of the recording window and behavioral task, the order of the temporal relationships among maximum velocity, maximum aperture, and minimum velocity hold constant. This study provides the basis for using a kinematic analysis approach in conjunction with existing behavioral tasks. Lastly, this study provides baseline performance of the unimpaired non-human primate model that can later be used to determine the timecourse of recovery in the spinal cord injury non-human primate model.

Introduction

Reaching and grasping tasks, mainly utilizing the Brinkman board described in chapter 1, are the primary method by which nonhuman primates with cervical spinal cord injury (SCI) are studied. These tasks mainly provide low resolution quantitative behavioral metrics to determine animal performance. As early as the 1980s, there were efforts in quantitatively assessing kinematic nonhuman primate performance during reach and grasp tasks. Some of these studies relied on specialized tasks involving the use of a manipulandum to determine hand velocity relationships [71], [72]. Later studies either relied on a post-hoc manual annotation technique using video editing software to track the nonhuman primate hand or taped physical markers to the animals' digits [73]–[77]. While time consuming and potentially influencing natural movement, these studies determined significant kinematic and temporal relationships. The main results from these studies uncovered the relationships between hand velocity and aperture (distance between index and thumb digits), the two digit approach shown in Figure 3.1 [78].

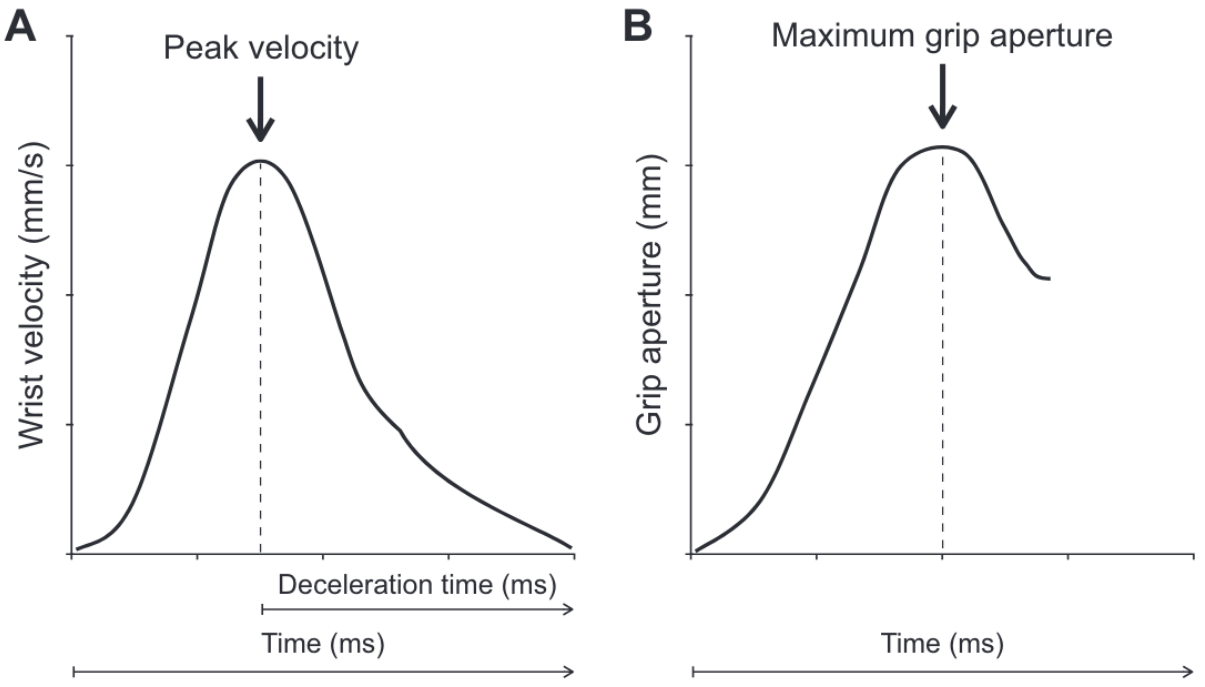

Figure 3.1. Two digit approach [68]. Characterization of reach and grasp through wrist velocity and aperture. In these experiments, the subject starts at a resting position and reaches toward a target reaching a maximum velocity between 51 – 54% into the movement. At the same time, their aperture (distance between index and thumb digit), increases, hits a maximum value 73 – 76% into the movement, then decreases upon reaching the target. It can also be seen that the minimum velocity occurs after the maximum aperture as the subject arrives at the target.

The two digit approach focuses on the temporal relationships between wrist velocity and maximum aperture. Roy et al. determined that maximum aperture is known to occur 73 - 76% into the reaching movement whereas peak velocity occurs 51 – 54% into the movement and is independent of object size [73], [75]. While not directly reported, it can also be inferred that the minimum velocity observed occurs after maximum aperture. Further studies by Satori et al. determined that peak velocity increased with distance covered, in accordance with the "isochrony principle" which states that the duration of voluntary movement remains constant across various distances [74], [78], [79]. These results are corroborated in seminal human works such as

Jeannerod and others, further emphasizing their importance as we relate nonhuman primate performance to human performance [77], [80]–[84].

Unfortunately, there is a limited amount of information regarding hand kinematics during the Brinkman board task. The previously discussed studies mainly focused on the animal in a sitting position or within the primate chair reaching for a food reinforcer [74]–[76], [76]. The timing relationships between velocity and aperture should be valid regardless of task. The missing knowledge will allow for additional quantitative metrics with a standardized task that is used ubiquitously, and which could be used to compare different studies directly. This study aims to quantify 2-dimensional hand kinematics and the timing relationships of the nonhuman primate model during the Brinkman board task using the apparatus from Chapter 2.

Methods

Animals

Two normal rhesus macaques (Macaca mulatta) one male (age: 4 years, 9 months; weight: 9.83 kg) and one female (age: 10 years, 5 months; weight: 9.48 kg) were recruited. The animals were housed at the California National Primate Research Center, Davis, CA; all primate procedures were approved by the California National Primate Research Center Institutional Animal Care and Use Committee.

Behavioral Task Design

Each animal was trained to use their right hand to retrieve food rewards from the wells on the Brinkman board. These rewards were varied to optimize the animal's motivation (e.g. yogurt covered raisins, nuts, etc.) but maintained a consistent dimensions. In the analysis described here, eight unique Brinkman boards were presented, which constituted one session. These Brinkman boards varied in the number of wells (1-9) and well orientation and followed a standardized Brinkman board task order as described in Chapter 1 and showing in Figure 1.3. Examples of these Brinkman boards are also shown in Figure 3.2. Once the animal successfully completed the

Brinkman board task only using the precision grip (using D1 and D2 to retrieve the food reinforcer), the animal was considered to be

proficient. Six different sessions held on two different days for each animal were recorded. Two food rewards were placed in the middle of the Brinkman board on each of the slopes.

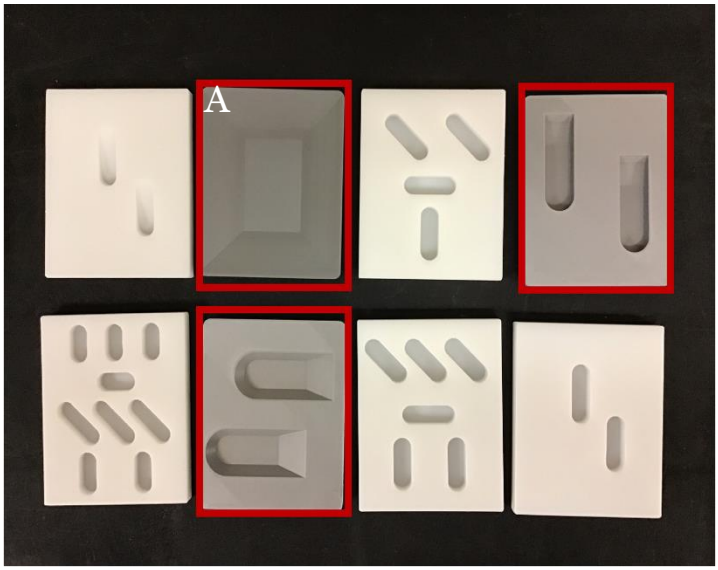

Figure 3.2. Standardized Brinkman board task. The order of the Remedial and Standard Brinkman boards was standardized. Completing all eight Brinkman boards consisted of one session. Both animals received all eight boards in the same order. After achieving proficiency, each animal was recorded for six Brinkman board sessions. **(A)** Remedial Brinkman board Level 1 used for kinematic analysis. This Brinkman board was used to limit the time where the digit is occluded.

Video Collection

Recording of the task started when the Brinkman board was presented to the animal and ended when the animal either successfully removed all the rewards from the Brinkman board or reached the 60 second timeout period. This process was repeated until the animal completed the total number of Brinkman boards (eight) for a given session. These videos were recorded at a resolution of 1920 x 1080 pixels at 120 frames per second in an MP4 format. The videos were then imported into DeepLabCut for further analysis.

DeepLabCut Analysis

After video collection, two DeepLabCut networks were trained using both the side and top mounted cameras, respectively. Videos using the Remedial Brinkman board Level 1 (Figure 3.2A) were used for this analysis. This minimized the time where the tips of the digits were occluded by being inside of the wells when retrieving the food reinforcer. These networks yielded test pixel errors of 11.25 (±0.1cm) and 30.31 (±0.22 cm). The process by which these networks were trained

is described in the methods section of Chapter 2. Table 3.1 describes the locations tracked using the side mounted DeepLabCut network.

Table 3.1. Locations of each digit tracked using the side mounted camera DeepLabCut network.

Feature	Locations
Thumb Digit (D1)	Fingertip, 1st Knuckle
Index Digit (D2)	Fingertip, 1st knuckle, 2nd knuckle
Middle Digit (D3)	Fingertip, 1st knuckle, 2nd knuckle
Ring Digit (D4)	Fingertip, 1st knuckle, 2nd knuckle
Pinky Digit (D5)	Fingertip, 1st knuckle, 2nd knuckle

Table 3.2 describes the locations tracked using the top mounted DeepLabCut network. Additional locations, the 3rd knuckle for D2-D5 and the 2nd knuckle of D1, were included for tracking.

Table 3.2. Locations of each digit tracked using the top mounted camera DeepLabCut network.

Feature	Locations
Thumb Digit (D1)	Fingertip, 1st Knuckle, 2nd knuckle
Index Digit (D2)	Fingertip, 1st knuckle, 2nd knuckle, 3rd knuckle
Middle Digit (D3)	Fingertip, 1st knuckle, 2nd knuckle, 3rd knuckle
Ring Digit (D4)	Fingertip, 1st knuckle, 2nd knuckle, 3rd knuckle
Pinky Digit (D5)	Fingertip, 1st knuckle, 2nd knuckle, 3rd knuckle

Outcome Measures

Using the tracking from DeepLabCut, kinematic and timing parameters were calculated. Table 3.3 below describes each outcome measure.

Table 3.3. Outcome measures list and description.	
Outcome	**Description**
Reaching Motion	The trajectory the primate's hand takes toward a food reward when its hand is visible and being tracked after the Brinkman board has been presented to the animal. Once the animal leaves the recording frame, the reaching motion is determined to have concluded.
Aperture	The Euclidean distance between the index and thumb digit tips when making the reach movement toward the food reward from the side mounted camera perspective. Measured in centimeters.
Max Aperture	The value where the Euclidean distance between the index and thumb digit tips when making the reaching movement towards the food reward hits a maximum. Measured in centimeters.
Hand Velocity	The speed with which the animal's hand moves when being tracked using the 2nd knuckle location from the middle digit from the top camera perspective. This begins when the hand enters frame and ends when the hand exits frame. Measured in centimeters per second.
Min Hand Velocity	The minimum speed the animal's hand moves during the reaching motion. Measured in centimeters per second.
Finger Extension	Determined by the distance from the 3rd knuckle to the distal locations (2nd knuckle, 1st knuckle and fingertip) with the index digit from the top camera perspective. Measured in centimeters.
Timing difference between maximum aperture and minimum velocity	The difference between the time of maximum aperture and the time of minimum velocity within a reaching motion. Measured in milliseconds.
Timing difference between maximum aperture and maximum finger extension	The difference between the time of maximum aperture and the time of maximum finger extension within a reaching motion. Measured in milliseconds.

Results

Two animals were trained and tested on the Remedial Brinkman board task, specifically using Remedial Brinkman board Level 1 as described in Aim 1. Two food reinforcers were placed in the middle of the well, as far apart as possible. This resulted in one food reinforcer being closer to the animal than the other. In some cases, the food reward shifted from its original location when it rolled while being placed inside the Camera Supporting Brinkman box described in Chapter 2.

Eleven reaching motions for Animal 1 and 10 reaching motions for Animal 2 were analyzed. One video was omitted from analysis due to poor tracking. Shown below are the outcome measures from Remedial Brinkman board Session 4 with Animal 1.

Aperture

Aperture is defined as the distance between the thumb and index fingertips, in centimeters, using the side mounted camera. Figure 3.3 shows the change in aperture movement during two reaching motions, shown in red or blue, based upon which food reinforcer was attempted first. In this Brinkman board session, Animal 1 first attempted to pick up the food reinforcer farther away. The digits start at approximately 2 cm apart and then expand to a maximum aperture of 3.67 cm. The aperture then decreases as the animal gets closer to the food reinforcers. Upon arrival, final adjustments to the aperture are made. Lastly, the animal retrieves it and quickly returns it to its mouth. The increase in aperture after retrieval is due to the animal's wrist rotation toward the camera. The wrist rotation causes the aperture distance to be exaggerated as this calculation is completed on a 2D plane.

A

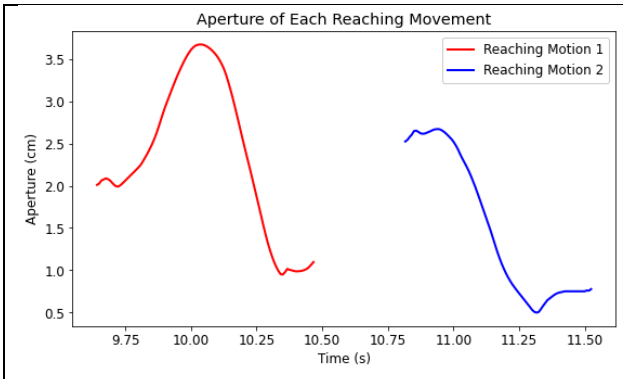

B

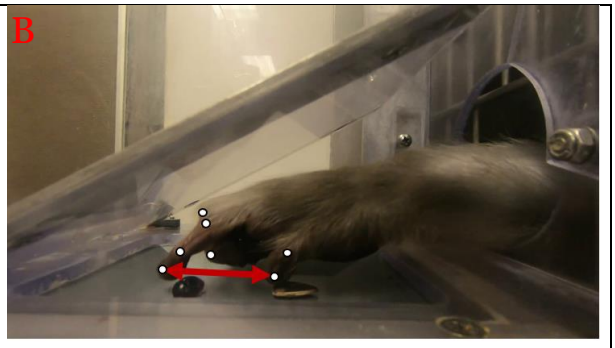

Figure 3.3. Aperture movements of Animal 1 during Remedial Brinkman board Session 4. **(A)** Aperture of Animal 1 by reaching motion. Aperture is defined as the distance between the thumb and index fingertips in centimeters. Two food reinforcers were placed on the board so that they were aligned in the middle of the board and were as far apart as possible. This resulted in one reinforcer being closer to the animal than the other. The aperture movement is broken down into one of two reaching motions, shown in red or blue, based upon which food reinforcer was attempted first. The maximum apertures during this session were 3.67 cm and 2.66 cm. **(B)** Video screenshot of maximum aperture of Animal 1 during Remedial Brinkman board Session 4.

During the second reaching motion, the animal reached a maximum aperture of 2.66 cm near the beginning of their recorded movement. Similar to the first reaching motion, the aperture decreased as the animal approached the food reinforcer and hit a minimum upon arrival.

Hand Velocity

The hand velocity was calculated using the top camera and the 2nd knuckle location of the middle digit. Figure 3.4 shows the hand velocity from Remedial Brinkman board Session 4. When the animal enters the frame, the hand is near or at maximum velocity. As the animal approaches the food reinforcer, their hand velocity decreases until it hits a minimum. This is approximately the time where the animal's index and thumb digits are making final adjustments to pick up the food reinforcers. After reaching a minimum velocity and retrieving the food reinforcer, the velocity then increases as the animal brings it back to their mouth. Out of frame, the animal eats the food reinforcer and makes a second reaching motion toward the second reinforcer.

Similar to the first reaching motion, the maximum velocity occurred close to when the hand is first in the frame. It then decreased as the animal approached the food reinforcers, hit a minimum near the reinforcer, then increased again as the animal moved their hand toward their mouth. As in the first reaching motion, the beginning and end of the reaching motion is not in the frame of the top mounted camera. This is also true of the side mounted camera.

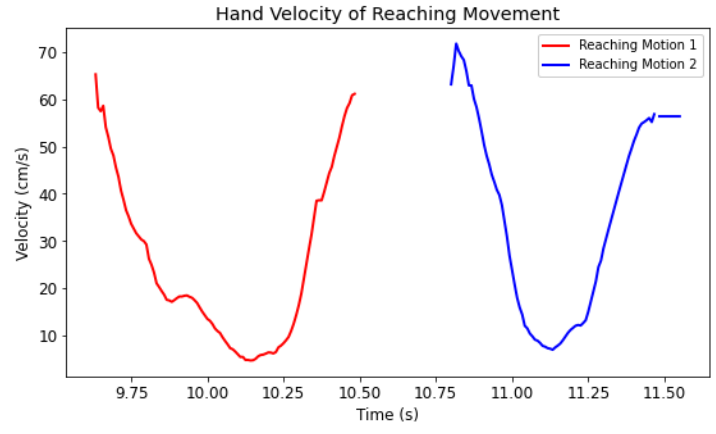

Figure 3.4 Hand velocity of Animal 1 during Remedial Brinkman board Session 4 separated by reaching movement. Hand velocity was calculated using the 2nd knuckle of the middle digit from the top camera perspective. The hand starts near or at maximum velocity and then decreases as the animal approaches the food reinforcer. Near the food reinforcer, the hand velocity reaches a minimum.

Finger Extension

Finger extension is defined as the distance between the 3rd knuckle of the index digit to the distal knuckles and fingertip. Figure 3.5A shows the finger extension by location on the index digit during the fourth Remedial Brinkman board session. Each location is designated a different color that corresponds to the physical location (blue = 3rd – fingertip, red = 3rd – 1st, and green = 3rd – 2nd). When the animal first comes into the frame, the index digit is not fully extended and only the 2nd knuckle location is tracked. The other two locations are occluded from the top camera. At approximately 10.1 seconds, the index digit is fully extended where all tracked locations can be seen. Figure 3.5B is a screenshot where the maximum finger extension occurs. The colors overlayed represent the same distances as the plot in Figure 3.5A.

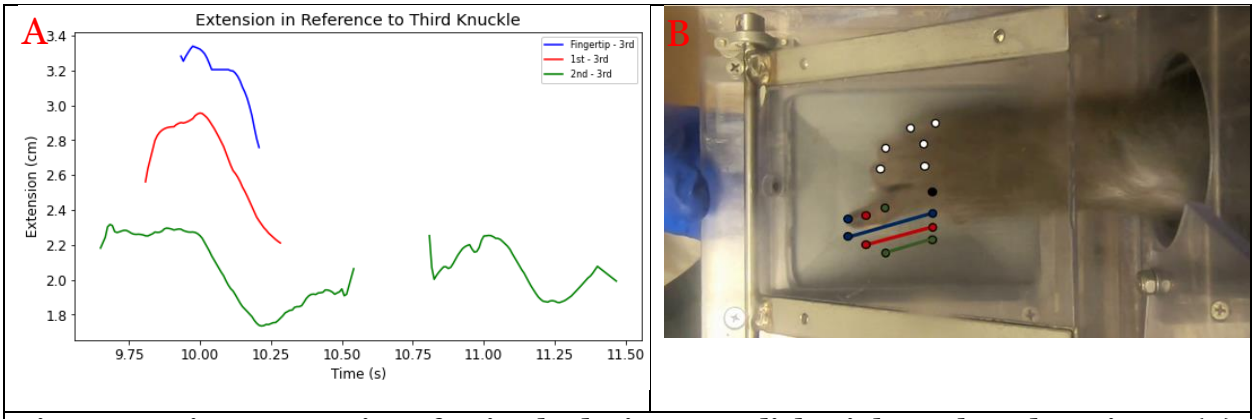

Figure 3.5. Finger Extension of Animal 1 during Remedial Brinkman board Session 4. (A) Finger extension from different locations on the index digit. Each color represents a different distance/location in reference to the 3rd knuckle (blue = 3rd – fingertip, red = 3rd – 1st knuckle, and green = 3rd – 2nd knuckle). When the animal first comes into the frame, the index digit is not at is fullest extension. The animal then reaches its fullest extension at approximately 10.1 seconds into the frame and then decreases after. The only location fully tracked is the 2nd knuckle location because the remaining locations are occluded from the top camera. This effect is shown in the second reaching motion where both the fingertip and 1st knuckle locations were not able to be tracked. **(B)** Video screenshot of maximum finger extension. The colors represent the distance depicted in Figure 3.5A.

After reaching maximum extension the index digit closes as the animal approaches the food reinforcers where it hits a minimum at approximately 10.35 seconds. Coincidentally, this is also the same timepoint where the animal's minimum aperture occurs or when the animal touches the

food reinforcer with both its index and thumb fingertips. Unlike the side mounted camera, the finger extension remains relatively constant upon exiting the frame.

In the second reaching motion, only the 2nd knuckle location is tracked as the other two locations are occluded from the top camera for the entirety of the reaching motion. Similar to the first reaching motion, there is a period of increased extension upon entering the frame followed by a period of decreased extension as the animal approaches the food reinforcers.

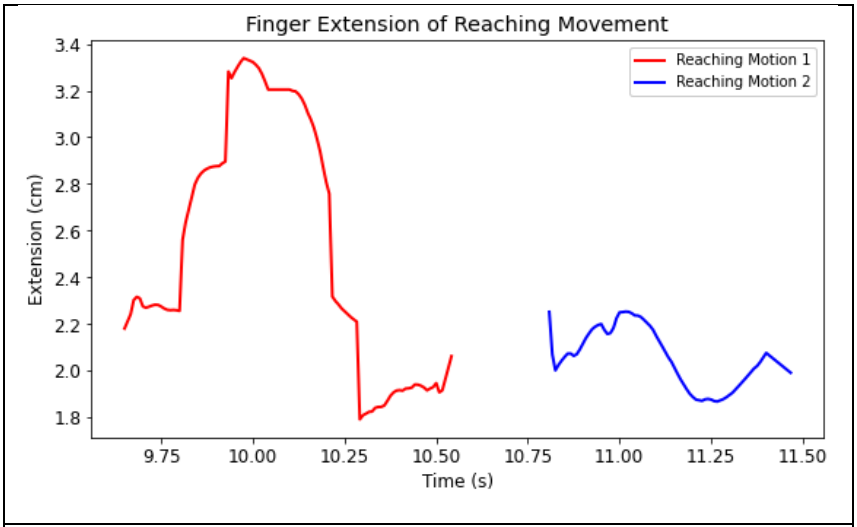

Figure 3.6. Overall finger extension during Remedial Brinkman board Session 4 by reaching motion. Using the finger extension by location, an overall finger extension plot was created from the maximum value from each. The large jumps, such as the two between 9.75 and 10 seconds, indicate timepoints where an additional location was no longer occluded from the top camera. In reaching motion 1, the maximum finger extension was 3.34 cm. In the second reaching motion, only the 2nd knuckle location was seen from the top camera, resulting in a maximum finger extension of 2.25 cm.

Using the locations, an overall finger extension plot was created using the maximum value from each location seen from the top camera. This is shown in Figure 3.6. The colors represent the reaching motions similar to Figures 3.3 and 3.4. These had maximum finger extensions of 3.34 cm for the first reaching motion and 2.25 cm for the second reaching motion.

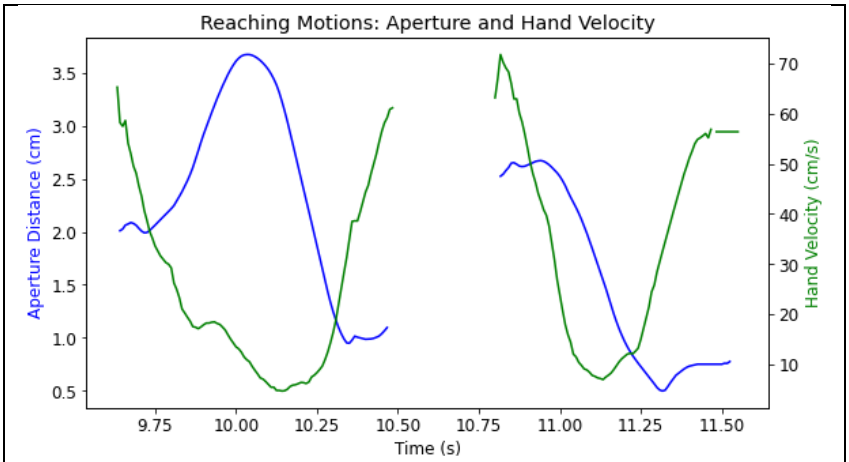

Figure 3.7. Dual axis aperture and hand velocity of Animal 1 during Remedial Brinkman board Session 4. Plotting these two outcomes together using the shared time axis allows for calculations between key parameters, in this case the time difference between maximum aperture and minimum velocity. These were 108 ms and 192 ms for the first and second reaching motion, respectively.

Aperture and Hand Velocity

The previous plots were plotted together using a shared time axis. From this plot, the timing between the maximum aperture and the minimum velocity was calculated during Remedial Brinkman board Session 4. These were determined to be 108 ms and 192 ms for the first and second reaching motion, respectively.

Aperture vs Overall Finger Extension

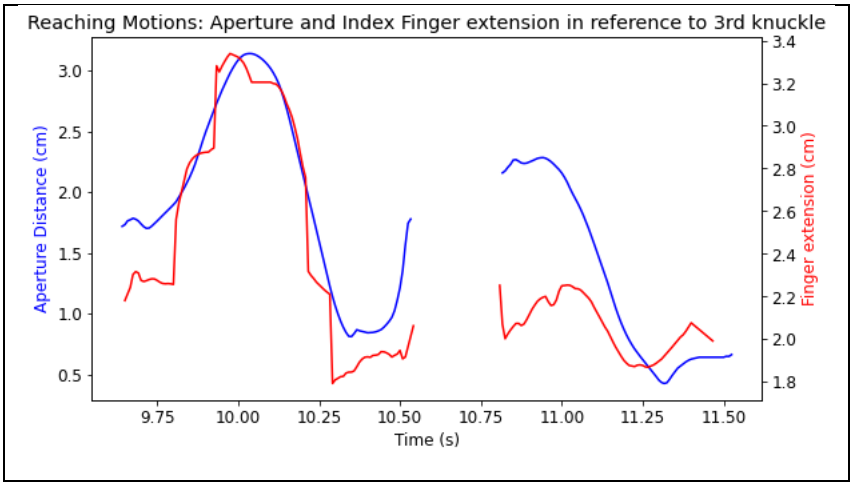

Figure 3.8. Dual axis aperture vs finger extension of Animal 1 during Remedial Brinkman board Session 4. In the first movement, finger extension occurs 58 ms before maximum aperture, and in the second movement finger extension occurs 92 ms after maximum aperture.

Aperture and overall finger extension were plotted together using a shared time axis. From this plot, the timing between maximum aperture and maximum finger extension was calculated during Remedial Brinkman board Session 4. These were determined to be -58 ms and 92 ms for the first and second reaching motion, respectively.

Velocity Data Results

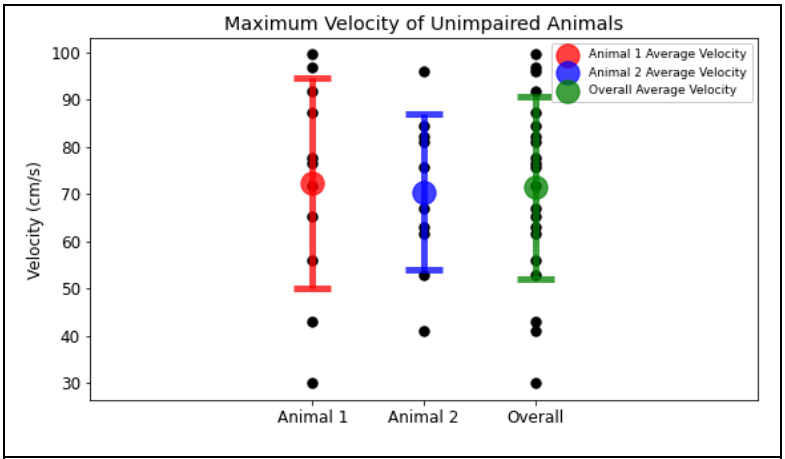

Figure 3.9. Average maximum hand velocity with scatterplot of datapoints by animal including overall result, which consisted of all reaching motions from both animals. This resulted in an overall average maximum velocity of 71.5 cm/s

Figure 3.9 is a summary plot of maximum velocity that includes Animal 1, Animal 2, and an overall plot including both animals' datasets in red, blue, and green, respectively. Combining both datasets yielded an overall average maximum velocity of 71.5 cm/s over 21 reaching motions.

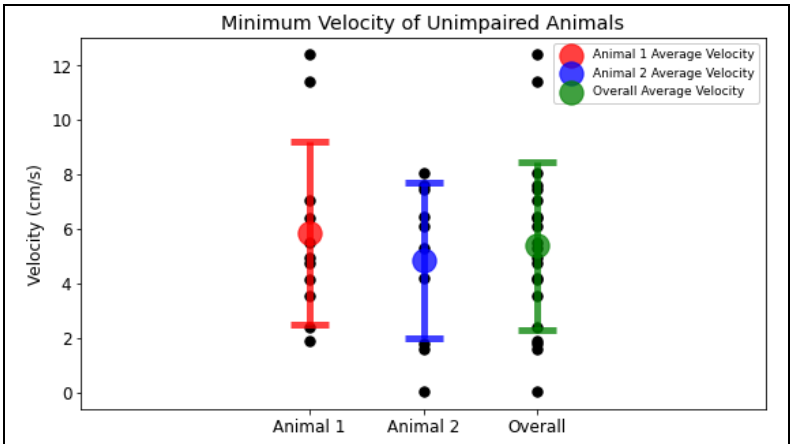

Figure 3.10. Average minimum hand velocity with scatterplot of datapoints by animal including overall result, which consisted of the entire dataset from both animals. This resulted in an overall average minimum velocity of 5.38 cm/s

Figure 3.10 is a summary plot of minimum velocity that includes Animal 1, Animal 2, and an overall plot including both animals' datasets in red, blue, and green, respectively. Combining both datasets yielded an overall average minimum velocity of 5.38 cm/s over 21 reaching motion.

Figure 3.11 includes the average time difference between maximum aperture and minimum velocity and maximum

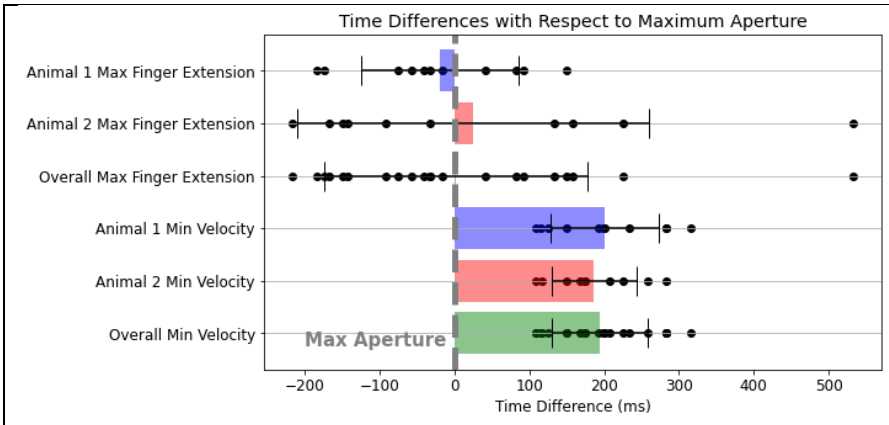

Figure 3.11. Average time difference between maximum aperture and finger extension and maximum aperture and minimum velocity for each animal with overall result. Animal 1 had an average time difference between maximum aperture and minimum velocity of 200.4 ms, and a time difference between maximum aperture and maximum finger extension of -19.6 ms. Animal 2 had an average time difference between maximum aperture and minimum velocity of 185.6 ms, and a time difference between maximum aperture and maximum finger extension of -24.8 ms. Overall, the average time difference between maximum aperture and minimum velocity was 193.8 ms, and the average time difference between maximum aperture and maximum finger extension was 1.57 ms.

aperture and maximum finger extension for each animal with the overall result appended. The overall consisted of all 21 reaching motions from both animals which resulted in an average time difference between maximum aperture and minimum velocity of 193.8 ms, and a time difference between maximum aperture and maximum finger extension of 1.57 ms. A Wilcoxon Ranked Sum test was applied to the overall dataset of both time difference datasets. The time difference between maximum aperture and minimum velocity was determined to be significant ($p<0.05$).

Table 3.4 includes average outcome measures for both animals over all reaching motions together.

Table 3.4. Summary table of averaged outcome measure for both animals over all reaching motions.

Outcome Measure	Value	Standard Deviation
Overall Average Maximum Aperture	2.49 cm	0.93 cm
Overall Average Maximum Finger Extension	2.77 cm	0.66 cm
Overall Average Maximum Hand Velocity	71.5 cm/s	19.3 cm/s
Overall Average Minimum Hand Velocity	5.38 cm/s	3.01 cm/s
Overall Average Time difference between maximum aperture and maximum finger extension	1.57 ms	176 ms
Overall Average Time difference between maximum aperture and minimum velocity	193.8 ms	64.2 ms

Discussion

Kinematic analysis of nonhuman primates can prove to be difficult with the use of physical markers or extensive manual annotation. In combination with DeepLabCut, kinematic analysis can be less time intensive and also remove the need for physical markers [85].

Hand Aperture

Figure 3.3 shows the two typical aperture curves seen with this analysis. In the first reaching motion, when the animal is attempting to grasp the food reinforcers that are further away, an initial opening can be seen with a distance of approximately 1.75 cm. This is the first time both digits are in the frame of the camera. The first movement recorded starts at 9.6 seconds.

As the animal approaches the food reinforcer, this value hits a maximum value of 3.13 cm at 10.03 seconds, or 43% into the first movement. This is different than Roy's results where maximum aperture occurs between 73 – 76% into the movement [73], [75], [76]. This difference is a result of methodology and the recorded movement. In Roy's testing methodology, the recording begins when the animal is at rest. Additionally, the animal at rest is visible to the camera. This is not the case in this study, where the focus of the camera is on the Brinkman board and the animal's starting position is not visibly recorded. This is also true of the second reaching motion where the maximum aperture of 2.28 cm occurs 25% into the movement. The only difference between the first and second reaching motion is the initial distance before maximum aperture occurs outside of the recorded window. Since the percentage is a function of when the animal is in the frame, the time within trials was reported and used for later analysis.

Average maximum aperture distance was determined to be 2.49 cm with a standard deviation of 0.93 cm. The average result is in accordance with previous studies, but the standard deviation could be interpreted to be high [75]. Upon reviewing the recordings it was determined that one animal had a potentially different reaching strategy, where the animal attempted to grab both

food reinforcers in one reaching motion. This animal was successful once in this strategy.

Lastly, there is a recording artifact at the end of the first reaching movement. After the animal retrieves the food reinforcer, the animal then turns their hand towards the camera. These results are based upon 2D kinematics which artificially inflate the aperture value. At first this seems undesirable, but it could be used to help determine when the animal rotates their hand upon returning it to their mouth. In the sample size recorded, this behavior is consistent with the food reinforcer placed farther away from the animal.

Velocity Results

Figure 3.4 shows the typical velocity profiles determined by this study. In both reaching motions, the animal is near or at maximum velocity upon entering the recording frame. Similar to the hand aperture, this result is different than that of previous studies due to methodological differences where maximum velocity occurs approximately halfway through the reaching motion. Due to this methodological difference, the minimum velocity value and timing was recorded to compare against aperture in later results. Average maximum velocity is in accordance with previous nonhuman primate and human studies [73], [78], [80], [84], [86].

Finger Extension

In discussions with primate experts, it was determined that hand extension is also an important metric to record. During the reaching movement, the index finger extends to create the distance between the index fingertip and the thumb (aperture). This measurement allows for the index digit to be isolated from the thumb digit movement. In this study finger extension was defined as the distance from the 3rd knuckle location to the distal locations, thus resulting in potentially three plots (as seen in Figure 3.5).

In the first reaching motion, the animal fully extends their index digit to retrieve the food reinforcer. This allows for every location on the digit to be seen from the top camera. In the second

reaching motion, the animal does not fully extend their digit and only the 2nd knuckle location can be seen. Since the location visible to the top camera varies, overall finger extension was determined as the maximal value of the most distal digit in view of the top camera. Given this limitation, there was no relationship between maximum finger extension and placement of the food reinforcer.

<u>Velocity and Maximum Aperture Temporal Relationship</u>

Temporal relationships in relation to maximum aperture results are seen in Figure 3.12. The average time difference between maximum aperture and minimum velocity was determined to be 193.8 ms, which was determined to be significant. The animal first reaching maximum aperture and then reaching a minimum velocity when making first contact with the food reinforcer intuitively makes sense. These results are similar to human studies in Furmanek, where the minimum velocity recorded occurs approximately 200 ms after maximum aperture [86]. This is seen in Figure 3.12.

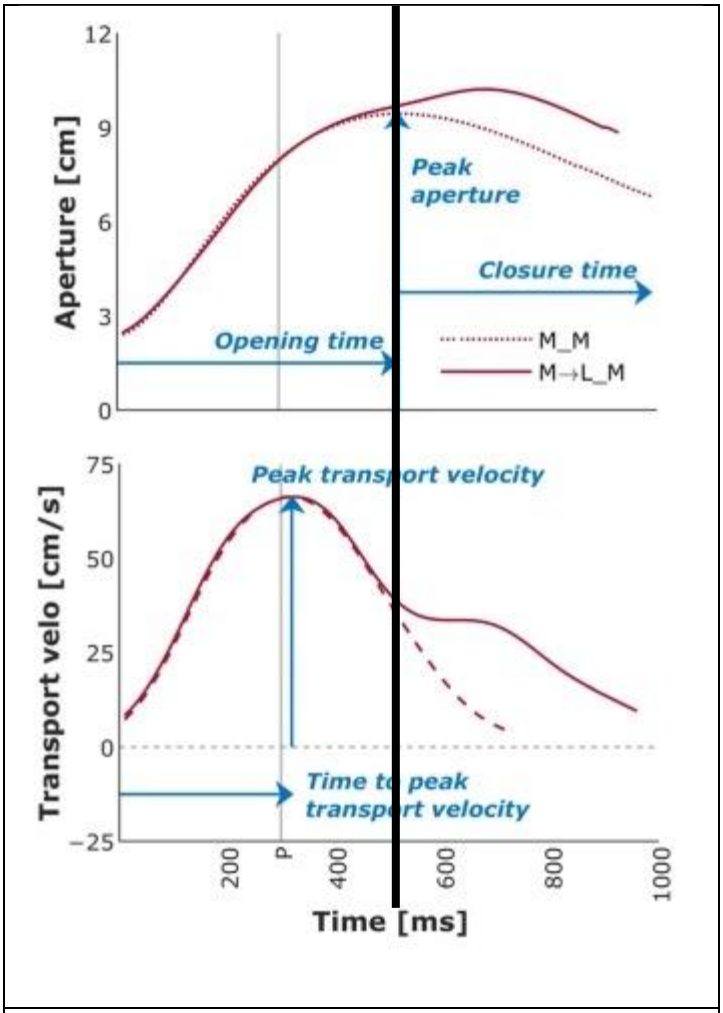

Figure 3.12. Temporal comparisons between transport velocity and aperture. Adapted from Furmanek et al. [86]. In this sample trial at baseline for human studies, peak transport velocity, which would translate to maximum velocity in this study, occurs first, then maximum aperture, and lastly minimum velocity. This occurs even if the size of the target changes (solid vs dashed line).

With respect to maximum velocity, no quantitative measurement was made due to the methodological differences, but it can be seen that maximum velocity recorded occurs before maximum aperture. These results are also seen in previous nonhuman primate works and seminal human studies [73], [75], [80], [84]. Regardless of the task, at baseline, the temporal order was as follows: maximum velocity, maximum aperture, minimum velocity. This can be seen in newer studies and datasets from Furmanek as seen in Figure 3.12 [86].

Finger Extension and Maximum Aperture Temporal Relationship

A similar analysis to velocity and maximum aperture was conducted for finger extension. Averaging over all reaching motions, it appears that maximum finger extension occurs at maximum aperture, but the variance is high at 176 ms. Looking at each animal independently, it can be seen that one animal's average time difference is slightly positive and the other's is slightly negative. Furthermore, in both animals maximum finger extension occurs both before and after maximum aperture. With the current dataset no temporal relationship can be found between maximum finger extension and maximum aperture.

Limitations

As previously stated, the main limitation of this study in comparison to previous studies is when the animal is within the camera frame. In previous studies, the animal at rest was seen and recorded by the camera. Additionally, the motion ended upon reaching the target. In this study, the animal is in motion upon entering the camera frame. Unlike previous studies, the initial portion of the return movement is recorded. This led to difficulties in making direct timing comparisons to previous studies. Despite these limitations, the temporal relationship between maximum aperture, maximum velocity and minimum velocity holds true.

Moving forward, to be aligned with previous studies the apparatus would need to be significantly modified. This would also provide the opportunity to move to three-dimensional kinematics, adding potential impacts and comparisons to human studies. This would also address the

limitation with using 2D kinematics, such as the artifact in Figures 3.3 and 3.7. The results from the Standard Brinkman board tasks in its current form allow for direct comparisons to previously studied animals within the International Primate Consortium. Significant changes to the task and apparatus could potentially make comparisons to historical data less impactful or impossible. Making any significant changes to the methodology and apparatus would not be possible, but it could be possible to create an additional apparatus. This would allow for both Standard Brinkman board tasks and an altered version of the apparatus from Chapter 2 to be implemented.

Another major limitation is that the food reinforcer was not consistent for each reaching movement. Every effort was made to keep the food reinforcers approximately the same size. Food reinforcers changed to maximize animal participation with the Brinkman board task. This is standard protocol for these animals.

Conclusion

Reach and grasp tasks such as the Brinkman board tasks are used in the nonhuman primate model, which primarily relies on low resolution quantitative analysis. Kinematic analysis provides a high-resolution solution in describing the specific aspects of the reaching motion, such as the temporal relationships between hand velocity and aperture. Existing unimpaired nonhuman primate literature focuses on these aspects without the use of the Brinkman board and has comparable results to the unimpaired human model. This study applies the kinematic analysis previously used in nonhuman primates and combines it with a physically markerless tracking system, DeepLabCut, and the Brinkman board task. These results suggest that kinematic analysis can be used with the Standard Brinkman board task and is also consistent with existing nonhuman primate and human studies regarding the temporal relationships between velocity and aperture.

Future Works

After determining baseline performance, it is possible to track these behaviors after spinal cord injury and during recovery. I expect that the timing relationship between maximum aperture and minimum velocity measure and maximum aperture will be sensitive to the spinal cord injury model. Over time, I hypothesized that both of these measures will recover over time, approaching baseline performance and maybe even reaching it. To begin to test this hypothesis, one animal was recruited and recorded. The animal was housed at the California National Primate Research Center, Davis, CA; all primate procedures were approved by the California National Primate Research Center Institutional Animal Care and Use Committee. The finger extension metric was not used in this analysis as no clear relationship between maximum finger extension and maximum aperture could be determined in the chapter 3 analysis. The results for this analysis are tabulated below in Table FW.1.

Table FW.1. Summary results of sample animal for the timecourse of recovery after spinal cord injury.

Brinkman board Attempt	Max Hand Velocity (cm/s)	Min Hand Velocity (cm/s)	Max Aperture (cm)	Time between max aperture and min velocity (ms)	Brinkman Board Score	Time of Completion(s)
Baseline	70	1.85	2.4	-267	3	3.32
Baseline	87.24	3.05	2.38	-133	3	3.32
Baseline	57.47	5.85	2.23	-325	3	3.31
Baseline	66.35	2.12	2.49	-333	3	3.31
1 Month Post	51.53	0.88	4.34	NaN	2	60
1 Month Post	71.33	1.355	3.86	NaN	1	60
2 Month Post	61.53	0	3.14	-1075	2	11.7
2 Month Post	45.23	2.96	3.96	-1142	2	11.7
3 Month Post	55.02	1.18	4.39	-942	3	6.96
3 Month Post	33.61	0.76	3.98	-567	2	6.96
4 Month Post	49.72	6.38	3.19	-308	2	8.51
4 Month Post	68.17	9.24	3.57	-292	2	8.51
9 Month Post	60.14	6.72	2.33	-75	3	18.58
9 Month Post	87.74	1.17	1.92	-58	3	18.58
End Date	60.25	5.63	2.54	-267	3	2.65
End Date	66.52	3.48	2.1	-408	3	2.65

From these results, several additional studies can be proposed. When comparing the kinematic results to the existing animals in Chapter 3, it can be seen that the timing relationship between maximum aperture and minimum velocity is outside the standard deviation while the maximum

and minimum velocity measures are within the standard deviation. This sample animal's timing relationship measures are overlayed on the existing baseline animals below.

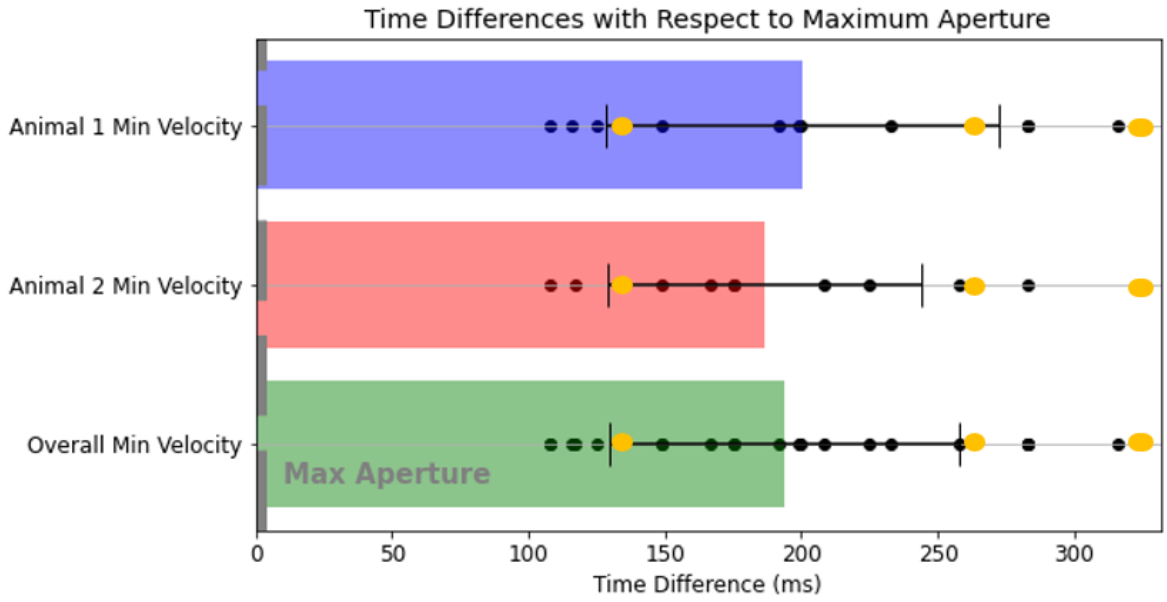

Figure FW.1. Sample Animal 1 baseline timing relationship between maximum aperture and minimum velocity overlayed on previous baseline results from Chapter 3. The bars represent the previous baseline data from Chapter 3 with the associated standard deviations. The yellow dots represent the four baseline reaching motions that were recorded before the sample animal's SCI. Three reaching motions exceed the standard deviation in the overall result. The four reaching motions averaged together results in an averaged time difference of -264.5 ms, also outside the standard deviation. From these results, it would be best to include additional baseline animals to better parse the maximum aperture and minimum velocity relationship.

This potentially indicates that the timing relationship measure could vary by animal or that there is not enough existing information to correctly parse out the timing relationship. I propose to increase the number of baseline animals to six, each with 12 reaching motions on the Level 1 Remedial Brinkman board. This would provide additional insights to this timing relationship to help determine that this sample animal and future animals are within baseline. Even with this increase of baseline results, when determining the sensitivity of this measure, the animals should be compared to their own baseline results.

In the sample animal with the selected time points, it appears that the timing relationship between the maximum aperture and minimum velocity metric is sensitive to injury and the following recovery. Additionally, it appears that maximum aperture is also sensitive to injury and recovery. Both have general improvement over time toward baseline performance after the initial decrease in performance. Given the sparseness of the data and lack of additional animals, no conclusions can be drawn. These results are promising and warrant additional study. To address the sparseness of the dataset, at least two Brinkman board sessions per month should be used for the analysis. This will parse out potential improvements in these two metrics. These collections should continue monthly until the animal's final Brinkman board session. This will also help determine at what timepoint the animal recovers most of their behavior. For example, by the four months post injury time point, the timing relationship metric appears to be fully recovered, but their maximum aperture seems to be high. By the nine-month post injury timepoint, both metrics appear to recover to baseline performance. The consistency of this performance will also need to be tested and recorded.

Looking forward, at least four additional animals should be collected to determine the sensitivity of these measures to recovery. Once these measures are proven to be sensitive to recovery, it could be possible to use these metrics to determine recovery in the presence of treatment. In this case, any reduction in recovery time to baseline with the inclusion of treatment would indicate that the treatment is effective.

References

[1] "VA Research on Spinal Cord Injury," p. 2.

[2] A. L. Natali, V. Reddy, and B. Bordoni, "Neuroanatomy, Corticospinal Cord Tract," in *StatPearls*, Treasure Island (FL): StatPearls Publishing, 2022. Accessed: Dec. 07, 2022. [Online]. Available: http://www.ncbi.nlm.nih.gov/books/NBK535423/

[3] K. L. Bunday, T. Tazoe, J. C. Rothwell, and M. A. Perez, "Subcortical Control of Precision Grip after Human Spinal Cord Injury," *J. Neurosci.*, vol. 34, no. 21, pp. 7341–7350, May 2014, doi: 10.1523/JNEUROSCI.0390-14.2014.

[4] K. L. Bunday and M. A. Perez, "Motor Recovery after Spinal Cord Injury Enhanced by Strengthening Corticospinal Synaptic Transmission," *Curr. Biol.*, vol. 22, no. 24, pp. 2355–2361, Dec. 2012, doi: 10.1016/j.cub.2012.10.046.

[5] S. N. Baker and M. A. Perez, "Reticulospinal Contributions to Gross Hand Function after Human Spinal Cord Injury," *J. Neurosci.*, vol. 37, no. 40, pp. 9778–9784, Oct. 2017, doi: 10.1523/JNEUROSCI.3368-16.2017.

[6] P. Federico and M. A. Perez, "Distinct Corticocortical Contributions to Human Precision and Power Grip," *Cereb. Cortex*, vol. 27, no. 11, pp. 5070–5082, Nov. 2017, doi: 10.1093/cercor/bhw291.

[7] E. S. Rosenzweig *et al.*, "Chondroitinase improves anatomical and functional outcomes after primate spinal cord injury," *Nat. Neurosci.*, vol. 22, no. 8, Art. no. 8, Aug. 2019, doi: 10.1038/s41593-019-0424-1.

[8] G. Courtine *et al.*, "Can experiments in nonhuman primates expedite the translation of treatments for spinal cord injury in humans?," *Nat. Med.*, vol. 13, no. 5, pp. 561–566, May 2007, doi: 10.1038/nm1595.

[9] J. P. Capitanio and M. E. Emborg, "Contributions of non-human primates to neuroscience research," *The Lancet*, vol. 371, no. 9618, pp. 1126–1135, Mar. 2008, doi: 10.1016/S0140-6736(08)60489-4.

[10] E. Taub, G. Uswatte, and T. Elbert, "New treatments in neurorehabiliation founded on basic research," *Nat. Rev. Neurosci.*, vol. 3, no. 3, pp. 228–236, Mar. 2002, doi: 10.1038/nrn754.

[11] N. A. Bayona, J. Bitensky, K. Salter, and R. Teasell, "The Role of Task-Specific Training in Rehabilitation Therapies," *Top. Stroke Rehabil.*, vol. 12, no. 3, pp. 58–65, Jul. 2005, doi: 10.1310/BQM5-6YGB-MVJ5-WVCR.

[12] C. Darian-Smith, "Monkey Models of Recovery of Voluntary Hand Movement After Spinal Cord and Dorsal Root Injury," *ILAR J.*, vol. 48, no. 4, pp. 396–410, Jan. 2007, doi: 10.1093/ilar.48.4.396.

[13] C. Darian-Smith and M. M. Ciferri, "Loss and recovery of voluntary hand movements in the macaque following a cervical dorsal rhizotomy," *J. Comp. Neurol.*, vol. 491, no. 1, pp. 27–45, Oct. 2005, doi: 10.1002/cne.20686.

[14] T. Isa, "Dexterous Hand Movements and Their Recovery After Central Nervous System Injury," *Annu. Rev. Neurosci.*, vol. 42, no. 1, pp. 315–335, Jul. 2019, doi: 10.1146/annurev-neuro-070918-050436.

[15] J. Won *et al.*, "Assessment of Hand Motor Function in a Non-human Primate Model of Ischemic Stroke," *Exp. Neurobiol.*, vol. 29, no. 4, pp. 300–313, Aug. 2020, doi: 10.5607/en20023.

[16] J. R. Napier, "The prehensile movements of the human hand," *J. Bone Joint Surg. Br.*, vol. 38-B, no. 4, pp. 902–913, Nov. 1956, doi: 10.1302/0301-620X.38B4.902.

[17] H. Klüver, "An Auto-Multi-Stimulation Reaction Board for Use with Sub-Human Primates," *J. Psychol.*, vol. 1, no. 1, pp. 123–127, Jan. 1935, doi: 10.1080/00223980.1935.9917246.

[18] M. Jeannerod, "The timing of natural prehension movements," *J. Mot. Behav.*, vol. 16, no. 3, pp. 235–254, Sep. 1984, doi: 10.1080/00222895.1984.10735319.

[19] M. Jeannerod, "The formation of finger grip during prehension. A cortically mediated visuomotor pattern," *Behav. Brain Res.*, vol. 19, no. 2, pp. 99–116, Feb. 1986, doi: 10.1016/0166-4328(86)90008-2.

[20] M. Santello, M. Flanders, and J. F. Soechting, "Patterns of Hand Motion during Grasping and the Influence of Sensory Guidance," *J. Neurosci.*, vol. 22, no. 4, pp. 1426–1435, Feb. 2002, doi: 10.1523/JNEUROSCI.22-04-01426.2002.

[21] S. A. Winges, D. J. Weber, and M. Santello, "The role of vision on hand preshaping during reach to grasp," *Exp. Brain Res.*, vol. 152, no. 4, pp. 489–498, Oct. 2003, doi: 10.1007/s00221-003-1571-9.

[22] E. Schmidlin *et al.*, "Behavioral Assessment of Manual Dexterity in Non-Human Primates," *J. Vis. Exp.*, no. 57, p. 3258, Nov. 2011, doi: 10.3791/3258.

[23] R. North *et al.*, “Quantifying the kinematic features of dexterous finger movements in nonhuman primates with markerless tracking,” *Rev.*, p. 6.
[24] I. Darian-Smith, K. Burman, and C. Darian-Smith, “Parallel pathways mediating manual dexterity in the macaque,” *Exp. Brain Res.*, vol. 128, no. 1–2, pp. 101–108, Sep. 1999, doi: 10.1007/s002210050824.
[25] M. P. Galea and I. Darian-Smith, “Manual dexterity and corticospinal connectivity following unilateral section of the cervical spinal cord in the macaque monkey,” *J. Comp. Neurol.*, vol. 381, no. 3, pp. 307–319, 1997, doi: 10.1002/(SICI)1096-9861(19970512)381:3<307::AID-CNE4>3.0.CO;2-6.
[26] J. Van der Harst and B. Spruijt, “Tools to measure and improve animal welfare: reward-related behaviour,” *Anim. Welf.*, vol. 16, no. 2, pp. 67–73, May 2007.
[27] S. J. Schapiro and S. P. Lambeth, “Control, Choice, and Assessments of the Value of Behavioral Management to Nonhuman Primates in Captivity,” *J. Appl. Anim. Welf. Sci.*, vol. 10, no. 1, pp. 39–47, Mar. 2007, doi: 10.1080/10888700701277345.
[28] G. Laule and M. Whittaker, “Enhancing Nonhuman Primate Care and Welfare Through the Use of Positive Reinforcement Training,” *J. Appl. Anim. Welf. Sci.*, vol. 10, no. 1, pp. 31–38, Mar. 2007, doi: 10.1080/10888700701277311.
[29] K. Coleman and A. Maier, “The use of positive reinforcement training to reduce stereotypic behavior in rhesus macaques,” *Appl. Anim. Behav. Sci.*, vol. 124, no. 3–4, pp. 142–148, May 2010, doi: 10.1016/j.applanim.2010.02.008.
[30] B. F. Skinner, *The behavior of organisms: an experimental analysis*. Oxford, England: Appleton-Century, 1938, p. 457.
[31] S. J. Schapiro, Ed., *Handbook of primate behavioral management*. Boca Raton: CRC Press, Taylor & Francis Group, 2017.
[32] Y. S. Nout *et al.*, “Animal Models of Neurologic Disorders: A Nonhuman Primate Model of Spinal Cord Injury,” *Neurotherapeutics*, vol. 9, no. 2, pp. 380–392, Apr. 2012, doi: 10.1007/s13311-012-0114-0.
[33] D. M. Basso, M. S. Beattie, and J. C. Bresnahan, “A Sensitive and Reliable Locomotor Rating Scale for Open Field Testing in Rats,” *J. Neurotrauma*, vol. 12, no. 1, pp. 1–21, Feb. 1995, doi: 10.1089/neu.1995.12.1.
[34] G. Courtine *et al.*, “Recovery of supraspinal control of stepping via indirect propriospinal relay connections after spinal cord injury,” *Nat. Med.*, vol. 14, no. 1, Art. no. 1, Jan. 2008, doi: 10.1038/nm1682.
[35] L. Friedli *et al.*, “Pronounced species divergence in corticospinal tract reorganization and functional recovery after lateralized spinal cord injury favors primates,” *Sci. Transl. Med.*, vol. 7, no. 302, p. 302ra134, Aug. 2015, doi: 10.1126/scitranslmed.aac5811.
[36] S. Kalsi-Ryan *et al.*, “The Graded Redefined Assessment of Strength Sensibility and Prehension: Reliability and Validity,” p. 15.
[37] S. Kalsi-Ryan, A. Curt, M. C. Verrier, and M. G. Fehlings, “Development of the Graded Redefined Assessment of Strength, Sensibility and Prehension (GRASSP): reviewing measurement specific to the upper limb in tetraplegia,” *J. Neurosurg. Spine*, vol. 17, no. 1 Suppl, pp. 65–76, Sep. 2012, doi: 10.3171/2012.6.AOSPINE1258.
[38] R. H. Jebsen, N. Taylor, R. B. Trieschmann, M. J. Trotter, and L. A. Howard, “An objective and standardized test of hand function,” *Arch. Phys. Med. Rehabil.*, vol. 50, no. 6, pp. 311–319, Jun. 1969.
[39] T. L. Moore, R. J. Killiany, M. A. Pessina, M. B. Moss, S. P. Finklestein, and D. L. Rosene, “Recovery from ischemia in the middle-aged brain: a nonhuman primate model,” *Neurobiol. Aging*, vol. 33, no. 3, p. 619.e9-619.e24, Mar. 2012, doi: 10.1016/j.neurobiolaging.2011.02.005.
[40] T. L. Moore, M. A. Pessina, S. P. Finklestein, B. C. Kramer, R. J. Killiany, and D. L. Rosene, “Recovery of fine motor performance after ischemic damage to motor cortex is facilitated by cell therapy in the rhesus monkey,” *Somatosens. Mot. Res.*, vol. 30, no. 4, pp. 185–196, Dec. 2013, doi: 10.3109/08990220.2013.790806.
[41] T. L. Moore *et al.*, “Inosine enhances recovery of grasp following cortical injury to the primary motor cortex of the rhesus monkey,” *Restor. Neurol. Neurosci.*, vol. 34, no. 5, pp. 827–848, Sep. 2016, doi: 10.3233/RNN-160661.
[42] A. R. Fugl-Meyer, L. Jääskö, I. Leyman, S. Olsson, and S. Steglind, “The post-stroke hemiplegic patient. 1. a method for evaluation of physical performance,” *Scand. J. Rehabil. Med.*, vol. 7, no. 1, pp. 13–31, 1975.

[43] I. Q. Whishaw, O. Suchowersky, L. Davis, J. Sarna, G. A. Metz, and S. M. Pellis, "Impairment of pronation, supination, and body co-ordination in reach-to-grasp tasks in human Parkinson's disease (PD) reveals homology to deficits in animal models," *Behav. Brain Res.*, vol. 133, no. 2, pp. 165–176, Jul. 2002, doi: 10.1016/S0166-4328(01)00479-X.
[44] J. Zhuang, W. Truccolo, C. Vargas-Irwin, and J. P. Donoghue, "Decoding 3-D Reach and Grasp Kinematics From High-Frequency Local Field Potentials in Primate Primary Motor Cortex," *IEEE Trans. Biomed. Eng.*, vol. 57, no. 7, pp. 1774–1784, Jul. 2010, doi: 10.1109/TBME.2010.2047015.
[45] C. Chen *et al.*, "Decoding grasp force profile from electrocorticography signals in non-human primate sensorimotor cortex," *Neurosci. Res.*, vol. 83, pp. 1–7, Jun. 2014, doi: 10.1016/j.neures.2014.03.010.
[46] H. Watanabe *et al.*, "Reconstruction of movement-related intracortical activity from micro-electrocorticogram array signals in monkey primary motor cortex," *J. Neural Eng.*, vol. 9, no. 3, p. 036006, May 2012, doi: 10.1088/1741-2560/9/3/036006.
[47] D. Shin *et al.*, "Prediction of Muscle Activities from Electrocorticograms in Primary Motor Cortex of Primates," *PLOS ONE*, vol. 7, no. 10, p. e47992, Oct. 2012, doi: 10.1371/journal.pone.0047992.
[48] C. Chen *et al.*, "Prediction of Hand Trajectory from Electrocorticography Signals in Primary Motor Cortex," *PLOS ONE*, vol. 8, no. 12, p. e83534, Dec. 2013, doi: 10.1371/journal.pone.0083534.
[49] A. Nakamura *et al.*, "Low-cost three-dimensional gait analysis system for mice with an infrared depth sensor," *Neurosci. Res.*, vol. 100, pp. 55–62, Nov. 2015, doi: 10.1016/j.neures.2015.06.006.
[50] J. Bailey, "Does the Stress of Laboratory Life and Experimentation on Animals Adversely Affect Research Data? A Critical Review," *Altern. Lab. Anim.*, vol. 46, no. 5, pp. 291–305, Nov. 2018, doi: 10.1177/026119291804600501.
[51] M. A. Pizzimenti *et al.*, "Measurement of Reaching Kinematics and Prehensile Dexterity in Nonhuman Primates," *J. Neurophysiol.*, vol. 98, no. 2, pp. 1015–1029, Aug. 2007, doi: 10.1152/jn.00354.2007.
[52] A. Mathis *et al.*, "DeepLabCut: markerless pose estimation of user-defined body parts with deep learning," *Nat. Neurosci.*, vol. 21, no. 9, pp. 1281–1289, Sep. 2018, doi: 10.1038/s41593-018-0209-y.
[53] L. Ruder, R. Schina, H. Kanodia, S. Valencia-Garcia, C. Pivetta, and S. Arber, "A functional map for diverse forelimb actions within brainstem circuitry," *Nature*, vol. 590, no. 7846, Art. no. 7846, Feb. 2021, doi: 10.1038/s41586-020-03080-z.
[54] R. Storchi *et al.*, "A High-Dimensional Quantification of Mouse Defensive Behaviors Reveals Enhanced Diversity and Stimulus Specificity," *Curr. Biol.*, vol. 30, no. 23, pp. 4619-4630.e5, Dec. 2020, doi: 10.1016/j.cub.2020.09.007.
[55] A. Bova, K. Kernodle, K. Mulligan, and D. Leventhal, "Automated Rat Single-Pellet Reaching with 3-Dimensional Reconstruction of Paw and Digit Trajectories," *J. Vis. Exp. JoVE*, no. 149, Jul. 2019, doi: 10.3791/59979.
[56] J. M. Barrett, M. G. R. Tapies, and G. M. G. Shepherd, "Manual dexterity of mice during food-handling involves the thumb and a set of fast basic movements," *PLOS ONE*, vol. 15, no. 1, p. e0226774, Jan. 2020, doi: 10.1371/journal.pone.0226774.
[57] R. North *et al.*, "Quantifying the kinematic features of dexterous finger movements in nonhuman primates with markerless tracking," in *2021 43rd Annual International Conference of the IEEE Engineering in Medicine & Biology Society (EMBC)*, Nov. 2021, pp. 6110–6115. doi: 10.1109/EMBC46164.2021.9630018.
[58] A. C. Roy, Y. Paulignan, A. Farnè, C. Jouffrais, and D. Boussaoud, "Hand kinematics during reaching and grasping in the macaque monkey," *Behav. Brain Res.*, vol. 117, no. 1–2, pp. 75–82, Dec. 2000, doi: 10.1016/S0166-4328(00)00284-9.
[59] "3D Video Tracking with CinePlex Behavioral Research System," *Plexon*. https://plexon.com/3d-video-tracking-cineplex-behavioral-research-system/ (accessed Mar. 23, 2022).
[60] G. Mahesh, "Image Deblurring Techniques - A Detail Review," *Int. J. Sci. Res. Sci. Eng. Technol.*, Jan. 2018.
[61] N. J. Kirkpatrick, R. J. Butera, and Y.-H. Chang, "DeepLabCut increases markerless tracking efficiency in X-ray video analysis of rodent locomotion," *J. Exp. Biol.*, vol. 225, no. 16, p. jeb244540, Aug. 2022, doi: 10.1242/jeb.244540.
[62] A. P. Georgopoulos, J. F. Kalaska, and J. T. Massey, "Spatial trajectories and reaction times of aimed movements: effects of practice, uncertainty, and change in target location," *J. Neurophysiol.*, vol. 46, no. 4, pp. 725–743, Oct. 1981, doi: 10.1152/jn.1981.46.4.725.
[63] A. Georgopoulos, J. Kalaska, R. Caminiti, and J. Massey, "On the relations between the direction of two-dimensional arm movements and cell discharge in primate motor cortex," *J. Neurosci.*, vol. 2, no. 11, pp. 1527–1537, Nov. 1982, doi: 10.1523/JNEUROSCI.02-11-01527.1982.

[64] L. Sartori, A. Camperio-Ciani, M. Bulgheroni, and U. Castiello, "How posture affects macaques' reach-to-grasp movements," *Exp. Brain Res.*, vol. 232, no. 3, pp. 919–925, Mar. 2014, doi: 10.1007/s00221-013-3804-x.
[65] A. C. Roy, Y. Paulignan, M. Meunier, and D. Boussaoud, "Prehension Movements in the Macaque Monkey: Effects of Object Size and Location," *J. Neurophysiol.*, vol. 88, no. 3, pp. 1491–1499, Sep. 2002, doi: 10.1152/jn.2002.88.3.1491.
[66] A. C. Roy, Y. Paulignan, M. Meunier, and D. Boussaoud, "Prehension movements in the macaque monkey: effects of perturbation of object size and location," *Exp. Brain Res.*, vol. 169, no. 2, pp. 182–193, Feb. 2006, doi: 10.1007/s00221-005-0133-8.
[67] M. I. Christel and A. Billard, "Comparison between macaques' and humans' kinematics of prehension: the role of morphological differences and control mechanisms," *Behav. Brain Res.*, vol. 131, no. 1, pp. 169–184, Apr. 2002, doi: 10.1016/S0166-4328(01)00372-2.
[68] U. Castiello and M. Dadda, "A review and consideration on the kinematics of reach-to-grasp movements in macaque monkeys," *J. Neurophysiol.*, vol. 121, no. 1, pp. 188–204, Jan. 2019, doi: 10.1152/jn.00598.2018.
[69] P. Viviani and G. McCollum, "The relation between linear extent and velocity in drawing movements," *Neuroscience*, vol. 10, no. 1, pp. 211–218, Sep. 1983, doi: 10.1016/0306-4522(83)90094-5.
[70] J. M. Karl and I. Q. Whishaw, "Different Evolutionary Origins for the Reach and the Grasp: An Explanation for Dual Visuomotor Channels in Primate Parietofrontal Cortex," *Front. Neurol.*, vol. 4, p. 208, Dec. 2013, doi: 10.3389/fneur.2013.00208.
[71] M. Gentilucci, U. Castiello, M. L. Corradini, M. Scarpa, C. Umiltà, and G. Rizzolatti, "Influence of different types of grasping on the transport component of prehension movements," *Neuropsychologia*, vol. 29, no. 5, pp. 361–378, 1991, doi: 10.1016/0028-3932(91)90025-4.
[72] M. P. Furmanek, M. Mangalam, M. Yarossi, K. Lockwood, and E. Tunik, "A kinematic and EMG dataset of online adjustment of reach-to-grasp movements to visual perturbations," *Sci. Data*, vol. 9, no. 1, Art. no. 1, Jan. 2022, doi: 10.1038/s41597-021-01107-2.
[73] G. Simon, G. Vakulya, and M. Rátosi, "The Way to Modern Shutter Speed Measurement Methods: A Historical Overview," *Sensors*, vol. 22, no. 5, Art. no. 5, Jan. 2022, doi: 10.3390/s22051871.
[74] S. Sagers and R. Patterson, "Shutter Speed in Digital Photography," p. 4.
[75] S. Wang, Y. Xu, Y. Zheng, M. Zhu, H. Yao, and Z. Xiao, "Tracking a Golf Ball With High-Speed Stereo Vision System," *IEEE Trans. Instrum. Meas.*, vol. 68, no. 8, pp. 2742–2754, Aug. 2019, doi: 10.1109/TIM.2018.2869180.
[76] J. Li, X. Long, D. Xu, Q. Gu, and I. Ishii, "An Ultrahigh-Speed Object Detection Method With Projection-Based Position Compensation," *IEEE Trans. Instrum. Meas.*, vol. 69, no. 7, pp. 4796–4806, Jul. 2020, doi: 10.1109/TIM.2019.2953418.
[77] N. O'Neill, K. M. Mah, A. Badillo-Martinez, V. Jann, J. L. Bixby, and V. P. Lemmon, "Markerless tracking enables distinction between strategic compensation and functional recovery after spinal cord injury," *Exp. Neurol.*, vol. 354, p. 114085, Aug. 2022, doi: 10.1016/j.expneurol.2022.114085.
[78] "Shutter Speed For Video – The Best Settings For Video," Jul. 23, 2021. https://jnrphotovideo.com/shutter-speed-for-video/ (accessed Mar. 24, 2022).
[79] A. Mathis, S. Schneider, J. Lauer, and M. W. Mathis, "A Primer on Motion Capture with Deep Learning: Principles, Pitfalls, and Perspectives," *Neuron*, vol. 108, no. 1, pp. 44–65, Oct. 2020, doi: 10.1016/j.neuron.2020.09.017.

Appendix 1

Animal 2 Results

Similarly to Animal 1, these plots were separated into three distinct time periods, “After SCI to Treatment”, “Treatment to Remedial”, and “Remedial Board Implementation”. The “After SCI to Treatment” section represents the time period when the animal was injured up to the point where the animal was given treatment for their injury. The nature of the treatment was unknown to the experimenter. The “Treatment to Remedial” section represents the time period after the animal’s treatment was started up to when the Remedial Brinkman boards were implemented into their daily testing. During this time period, the animal was expected to recover over time. Lastly, “Remedial Board Implementation” represents the time period where the Remedial Brinkman boards were given to the animals on a regular basis. The rolling time period was determined for each section.

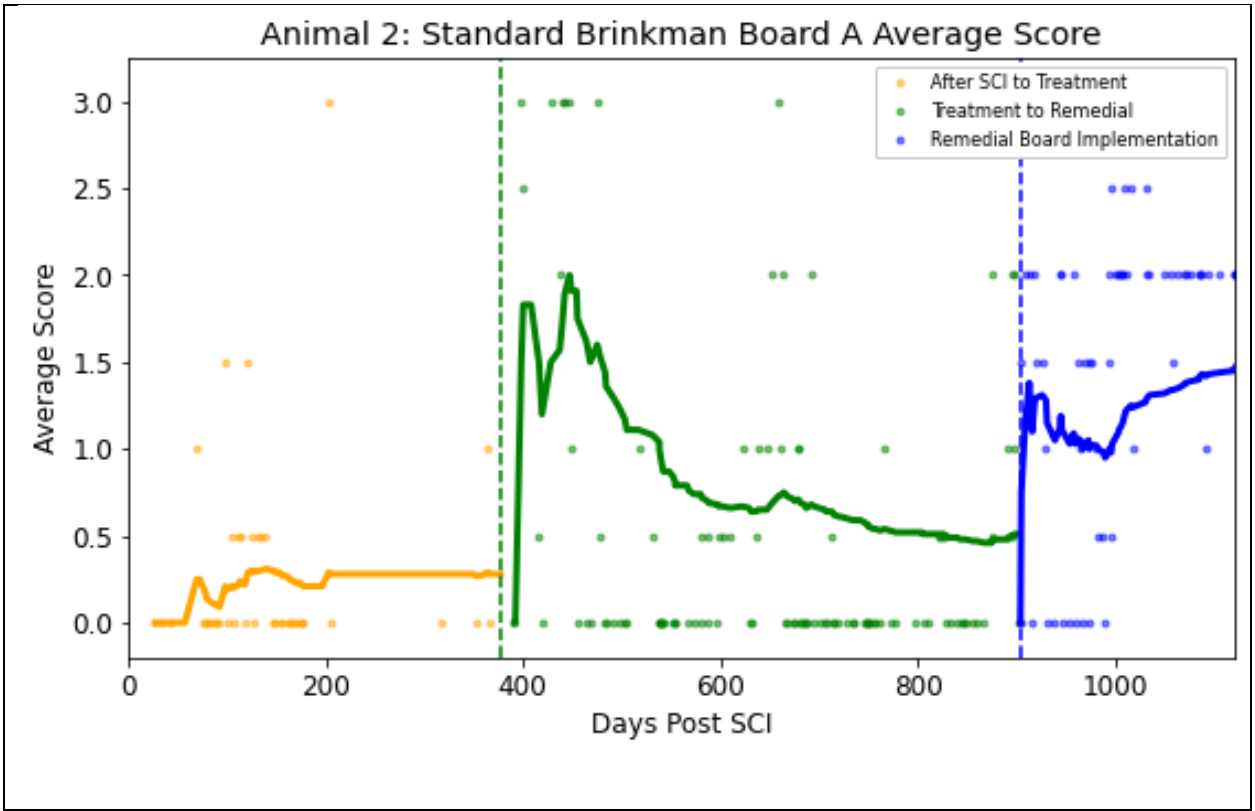

Figure A1.1. Animal 2 Standard Brinkman board A score. The three different colors represent three different time periods (yellow: After SCI to Treatment; green: Treatment to Remedial, blue; Remedial Board Implementation). The individual dots represent the average score on a given day. The rolling average for each section was calculated and represented by the solid line in their respective colors.

The final average scores for the "After SCI to Treatment", "Treatment to Remedial" and "Remedial Board Implementation" sections were 0.28, 0.51, and 1.47. A causal impact analysis was conducted between the "Treatment to Remedial" and the "Remedial Board Implementation" sections to determine the effectiveness of the Remedial Brinkman boards. The Remedial Brinkman boards were shown to have a significant positive effect (probability <0.05).

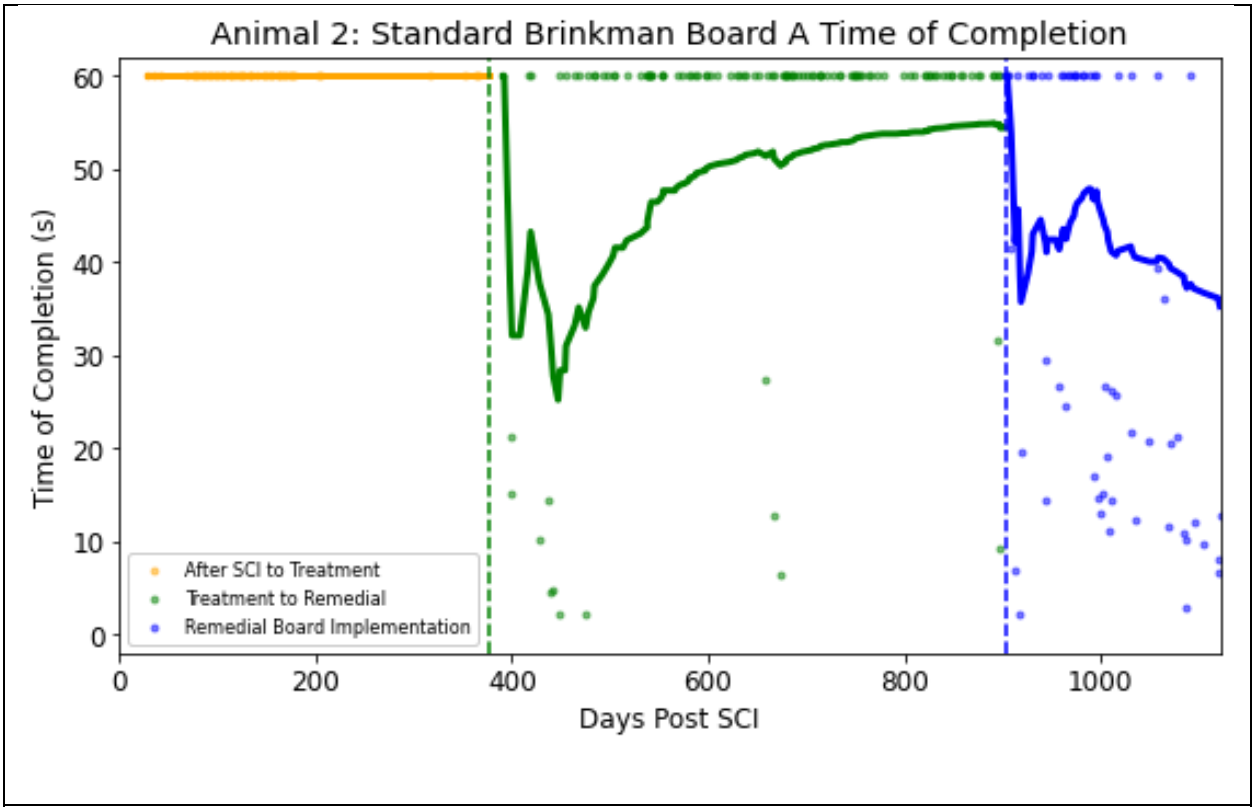

Figure A1.2. Animal 2 Standard Brinkman board A time of completion. The three different colors represent three different time periods (yellow: After SCI to Treatment; green: Treatment to Remedial; blue: Remedial Board Implementation). The individual dots represent the time of completion on a given day. The rolling average for each section was calculated and represented by the line in their respective colors.

The final time of completion scores for the "After SCI to Treatment", "Treatment to Remedial" and "Remedial Board Implementation" sections were 60 seconds, 54.48 seconds, and 35.27 seconds. A causal impact analysis was conducted between the "Treatment to Remedial" and the "Remedial Board Implementation" sections to determine the effectiveness of the Remedial Brinkman boards. The Remedial Brinkman boards were shown to have a significant positive effect (probability <0.05).

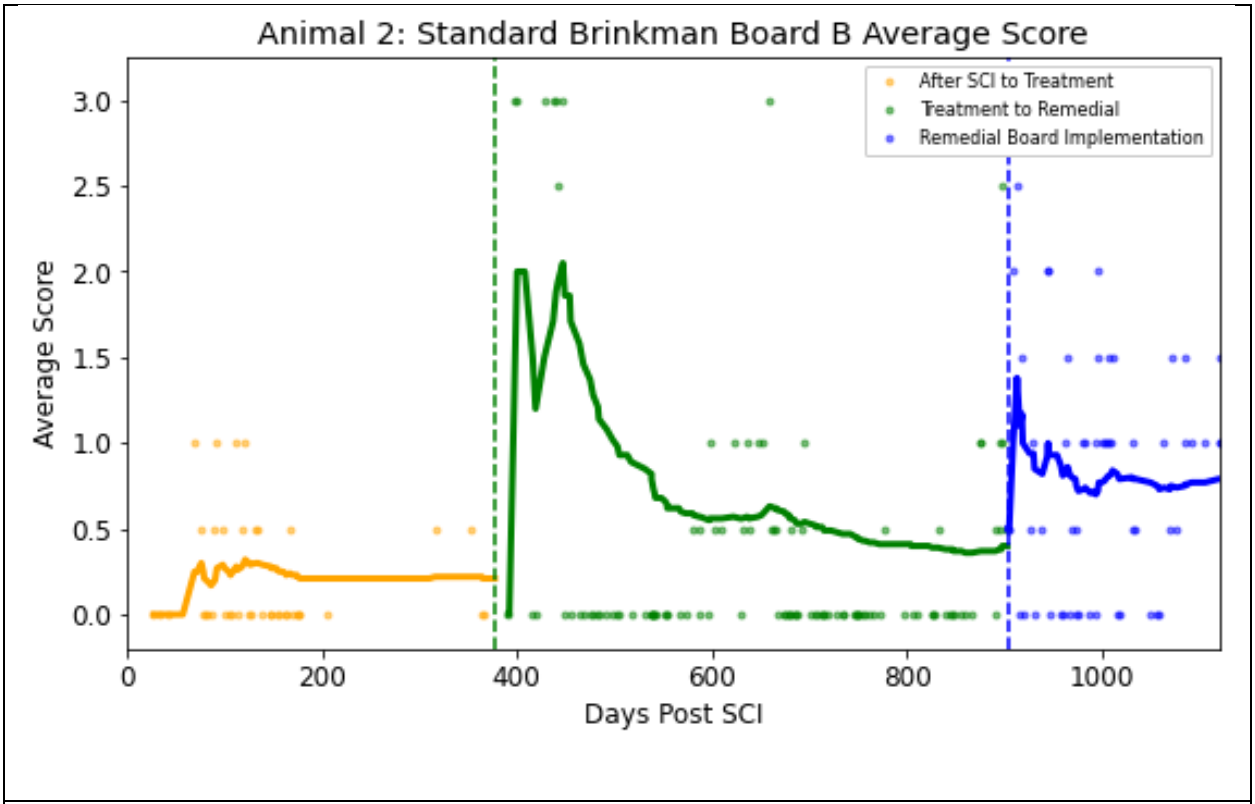

Figure A1.3. **Animal 2 Standard Brinkman board B score.** The three different colors represent three different time periods (yellow: After SCI to Treatment; green: Treatment to Remedial; blue: Remedial Board Implementation). The individual dots represent the average score on a given day. The rolling average for each section was calculated and represented by the line in their respective colors.

The final average scores for the "After SCI to Treatment", "Treatment to Remedial" and "Remedial Board Implementation" sections were 0.21, 0.40, and 0.79. A causal impact analysis was conducted between the "Treatment to Remedial" and the "Remedial Board Implementation" sections to determine the effectiveness of the Remedial Brinkman boards. The Remedial Brinkman boards were shown to have a significant positive effect (probability <0.05).

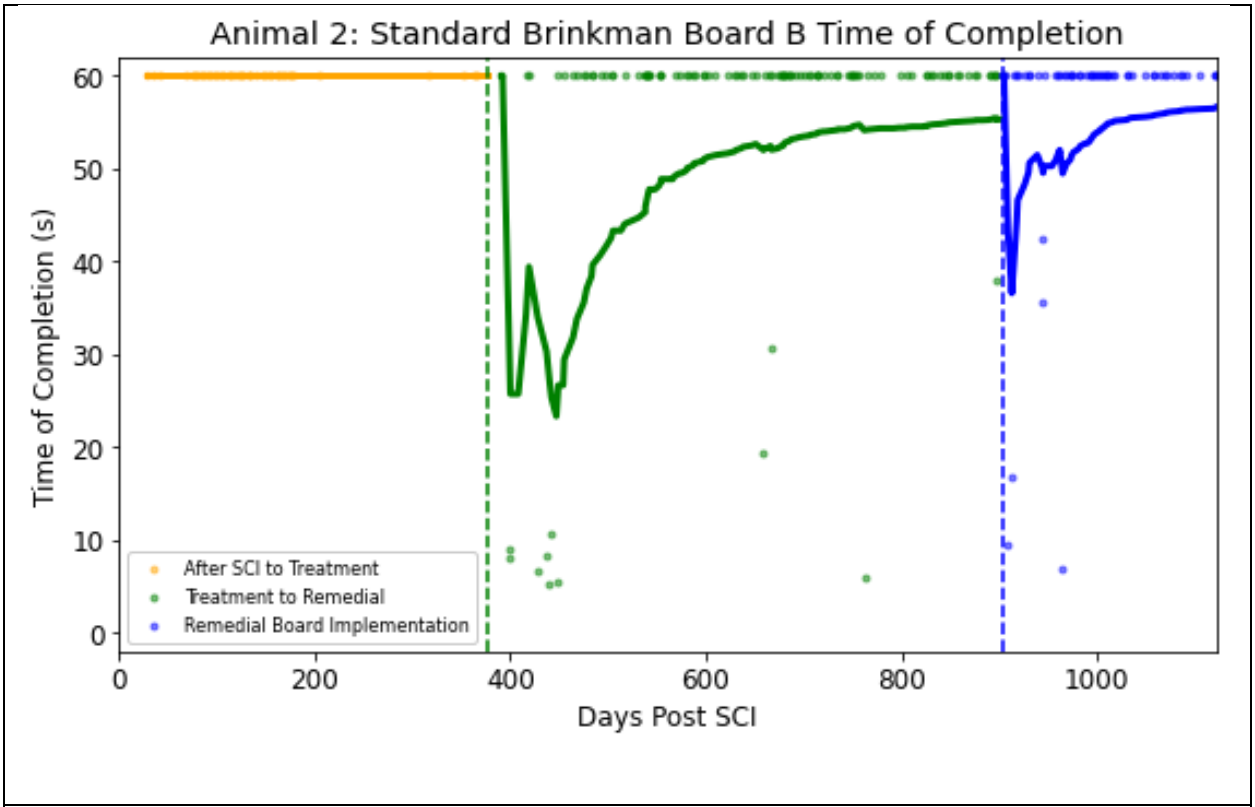

Figure A1.4. Animal 2 Standard Brinkman board B time of completion. The three different colors represent three different time periods (yellow: After SCI to Treatment; green: Treatment to Remedial; blue: Remedial Board Implementation). The individual dots represent the time of completion on a given day. The rolling average for each section was calculated and represented by the line in their respective colors.

The final time of completion scores for the "After SCI to Treatment", "Treatment to Remedial" and "Remedial Board Implementation" sections were 60 seconds, 54.34 seconds, and 56.63 seconds for Animal 2 using Standard Brinkman board B. A causal impact analysis was conducted between the "Treatment to Remedial" and the "Remedial Board Implementation" sections to determine the effectiveness of the Remedial Brinkman boards. The Remedial Brinkman boards were shown to have no effect.

Animal 2 Count Data Results:

Count data was collected based on Animal 2's performance using Standard Brinkman boards A and B. From Table A1.1, a score of 0 represents no attempt from Animal 2. The total number of 0 scores were tallied, and a percentage of 0 scores was calculated based upon the time period in

which they occurred. Similarly, the number of times the animal had a 60 second timeout (did not clear the Standard Brinkman board in the allotted time or did not participate) was also tallied. The percentage of timeouts was calculated based on the time period in which they occurred.

Table A1.1. Animal 2 Standard Brinkman board A 0 Score Counter.

Time Frame	0 Score Trials	Total Trials	Percentage of 0 score
After SCI to Treatment	29	41	70.73
Treatment to Remedial	99	112	88.39
Remedial Brinkman Implementation	24	60	40

Table A1.2. Animal 2 Standard Brinkman Board B 0 score counter.

Time Frame	0 Score Trials	Total Trials	Percentage of 0 score
After SCI to Treatment	27	40	67.5
Treatment to Remedial	74	109	67.89
Remedial Brinkman Implementation	16	56	28.57

Table A1.3. Animal 2 Standard Brinkman Board A 60 Second Time of Completion Counter.

Time Frame	60 Second Trials	Total Trials	Percentage of 60 Second Trials
After SCI to Treatment	41	41	100
Treatment to Remedial	99	112	88.39
Remedial Brinkman Implementation	10	60	16.67

Table A1.4. Animal 2 Standard Brinkman Board B 60 Second Time of Completion Counter.			
Time Frame	60 Second Trials	Total Trials	Percentage of 60 Second Trials
After SCI to Treatment	40	40	100
Treatment to Remedial	99	109	90.83
Remedial Brinkman Implementation	51	56	91.07

From this count data, a proportional z test was conducted. The z statistic and resulting p values are tabulated in Table A1.5 below. All metrics except Standard Brinkman board B time of completion were determined to be significant. This would suggest that the Remedial Brinkman boards do have a positive impact in this animal.

Table A1.5. Animal 2 Proportional Z test Results between Treatment to Remedial and Remedial Board Implementation Sections.		
Board	Z- Statistic	P value
Standard Brinkman board A Score	5.61	P<0.001
Standard Brinkman board B Score	6.7	P<0.001
Standard Brinkman board A Time of Completion	4.8	P<0.001
Standard Brinkman board B Time of Completion	-0.05	P=0.52

Remedial Brinkman Board Difficulty Commentary

An assumption of the Remedial Brinkman boards is that they are easier to complete than the Standard Brinkman boards. This can be tested by directly comparing completion time among the Brinkman boards. A lower time of completion would indicate that the board is easier to complete. Median time of completion for six animals was collected on the various types of Brinkman boards as described in the Chapter 1 Protocol section. These results are shown below in Table A1.6.

Table A1.6. Median time of completion scores by animal and Brinkman board type. The average was calculated by Brinkman board type.					
Animal	Standard A	Standard B	Remedial 1	Remedial 2V	Remedial 2H
Animal 1	10.07 s	32.56 s	7.33 s	7.36 s	7.77 s
Animal 2	7.16 s	60 s	6.85 s	6.84 s	7.70 s
Animal 3	30.13 s	25.7 s	14.46 s	19.67 s	13.46 s
Animal 4	7.08 s	5.95 s	4.93 s	6.08 s	5.06 s
Animal 5	10.05 s	13.16 s	9.18 s	9.62 s	8.98 s
Animal 6	60 s	60 s	18.09 s	23.79 s	18.12 s
Average	20.75 s	32.90 s	10.12 s	12.23 s	10.18 s

Figure A1.5 shows the group results using the averaged median time of completions for each two food reward Brinkman boards. The two Standard Brinkman boards (red bars) and the three Remedial Brinkman boards (blue bars) are shown. Individual datapoints and the standard deviation are shown by the dot above the bar.

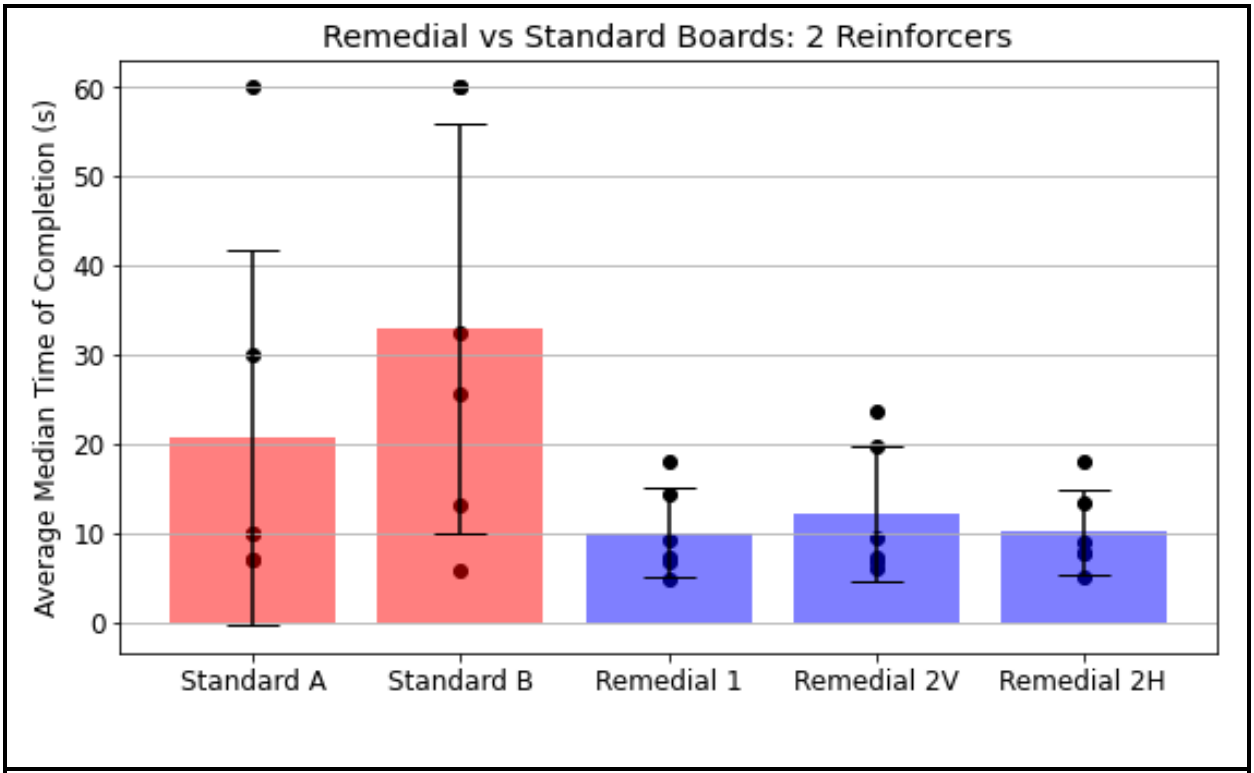

Figure A1.5. Averaged median time of completions across six animals by Brinkman board type with maximum two food rewards. The red bars are the Standard Brinkman boards and the blue bars are the Remedial Brinkman boards. Individual data points and standard deviation are shown by the dot above the bar. For Standard Brinkman board A (Standard A) two animals had a 60 second median time of completion score and another two animals overlap at 10 seconds. For Standard Brinkman board B, two animals had a 60 second median time of completion.

A Flinger-Killen test was conducted to determine whether the variance of the Brinkman boards is the same based upon comparison group. This nonparametric test was used due to the small sample size per Brinkman board and its robustness against non-normal distributions. P-values below 0.05 were deemed significant.

Table A1.7. Flinger-Killen test for equality of variance.

Comparison	Statistic	P- value
All Groups	14.37	0.006
Standard A vs Remedial boards	14.82	0.002
Standard B vs Remedial boards	8.272	0.041
Remedial boards only	2.83	0.243
Standard boards only	0.072	0.789

Three of the five comparisons were deemed significant (all groups $p<0.05$, Standard A vs Remedial boards $p<0.05$, and Standard B vs Remedial boards $p<0.05$). There was no statistical difference among the Remedial Brinkman boards or the between the Standard Brinkman boards. These results show that the Remedial boards are easier to complete than the Standard Brinkman boards. They also suggest that overall, there is low to no discernable difference among the Remedial Brinkman boards. Lastly, these results show no discernable difference between the Standard Brinkman boards, suggesting that the inclusion of one sloped edge is insignificant or ineffective in decreasing the difficulty of the task.

Appendix 2

Motion Blur During Recording Commentary

Regarding the speed of the movement, the faster the animal moves within a reaching movement, the more likely the frame is to blur. This effect is likely due to the exposure time (or shutter speed) being too long. The exposure time is the length of time the sensor is exposed to incoming light to create an image [64], [65]. The longer the exposure time, the more the image is blurred [64], [65]. Figure A2.1B is an example of significant motion blur when recording the nonhuman primate hands, while Figure A2.1A has limited motion blur.

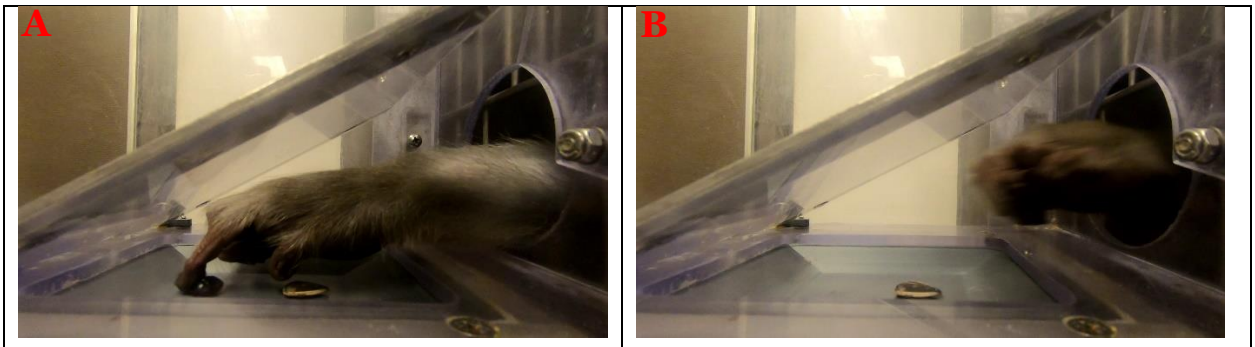

Figure A2.1A. **Nonhuman primate hand during Brinkman board task. Figure A2.1(A)**. Limited motion blur image of nonhuman primate hand during the Brinkman board task. The index digit is currently in contact with the food reward with the thumb digit closing in. Both digits of interest, the index and thumb digits, are clearly visible and blurring is at a minimum. This would allow for manual annotation to be relatively straightforward. **(Figure A2.1B)**. Significantly blurred image of nonhuman primate during the Brinkman board task. The hand is moving toward the animal's mouth in possession of the food reward. The individual digits are difficult to discern, and the food reward cannot be clearly seen. In motion and to the human eye, this frame would appear normal. To a neural network, the image would appear to be unique and could be a potential source of error. During the manual annotation phase, this would be difficult to annotate properly, leading to another potential source of error.

It has been previously shown that object detection methods, similar to ones used in DeepLabCut, perform more favorably with limited motion blur [66]–[68]. This allows for a more consistent labelling of landmarks. When the motion blur is significant, it can introduce large errors during manual or automatic annotation. To reduce this type of error it's advisable not to manually label these types of frames, as it can have the added effect of the neural network "skipping" automatic

annotation of similar frames with large amounts of motion blur.

With the frames unlabeled, it becomes difficult to discern the true location of these landmarks solely from the dataset; only estimated location based upon the known locations would be feasible. One possible solution to avoid this would be to limit the number of frames subjected to significant motion blur through decreasing the exposure time upon recording. Reducing the exposure time can result in sharper images, reducing motion blur. Figure A2.2 details the relationship between exposure time (shutter speed) and image sharpness.

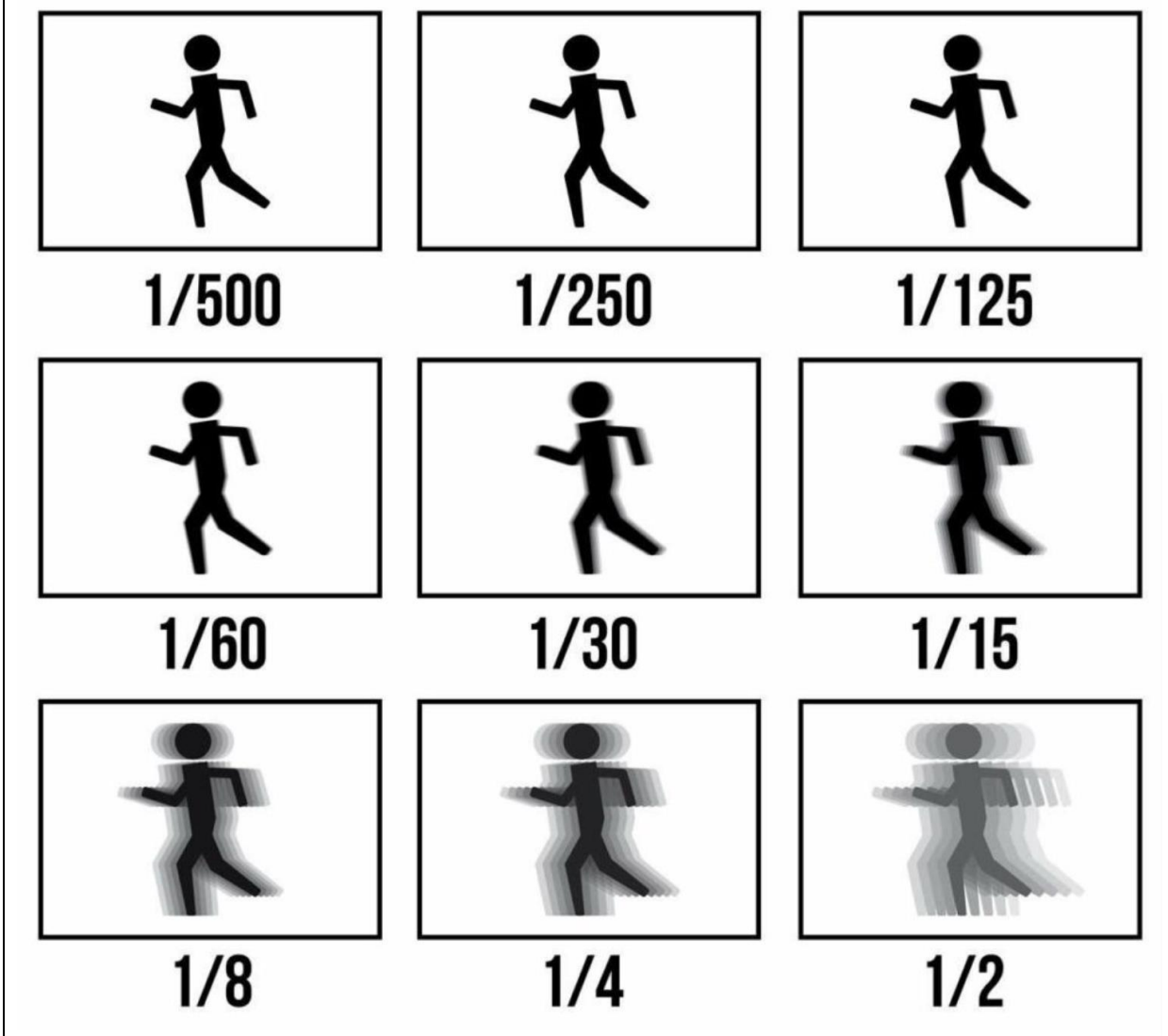

Figure A2.2. Relationship between exposure time/shutter speed and image sharpness. Figure adapted from Jeff Photography [69]. The same image is presented in each of the frames with a corresponding shutter speed in fractions of a second. As this value decreases, the amount of light hitting the lens also decreases. This results in a sharper image with less motion blur. For example, the ½ shutter speed has significant motion blur with a shadowing effect that precedes and trails the object. In sharp contrast, the 1/500 shutter speed image appears sharp.

Figure A2.2 shows that reducing the exposure time/shutter speed can significantly reduce the amount of motion blur and increase the sharpness of the image. To compare the extremes, the ½ second shutter speed has significant motion blur. It is difficult to discern the individual appendages of the stick figure. It appears as if the image is "smeared" as indicated by the leading

and trailing shadows. Comparing the ½ second shutter speed to the 1/500 second shutter speed, the image no longer exhibits the same blurring, appearing much sharper.

A substantial side effect upon recording at high shutter speeds is the video appearing jagged, rigid, and unnatural to the human eye [64]. This could potentially limit any additional qualitative information that could be interpreted from these videos outside of this analysis. For example, these videos would be difficult to understand in a presentation format. To best balance out this effect, there must be correct ISO balance for the camera's sensitivity to the light in the environment. If changing the recording settings is not possible, motion blur in the video can be reduced post hoc with software, such as Adobe Premiere Pro using deconvolution with a Gaussian filter [62]. Mehesh compares and contrasts additional sharpening and deblurring techniques that could be potentially suitable for these videos [62].

Differences in Pixel Error Between DeepLabCut Paper and Nonhuman Primate Use Case.

When training a DeepLabCut network, the network is evaluated on its accuracy using a root mean square error [52]. This is done by using the remaining 10% of frames that the network is naïve to and comparing the human annotated response to the network's automated annotated response.

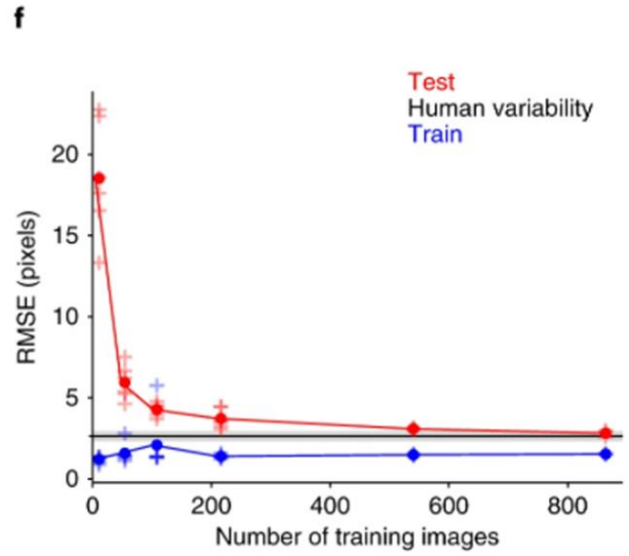

Figure A2.3. Relationship between number of training images and accuracy based upon the root mean square error, adapted from Mathis et al. [52]. Generally, more training images lead to a lower RSME as seen by the red curve representing the test data set. This is balanced with the time required to annotate and create these training images. This is how the number of frames for each network was determined.

When comparing the resulting nonhuman primate networks to Figure A2.3 it can be seen that the root mean pixel error is significantly higher when comparing a similar number of annotated frames; the number of annotated frames was originally decided from Figure A2.3 The higher root mean square error was persistent through the additional nonhuman primate DeepLabCut networks that were trained, and not explicitly described in the Methods section. These errors are shown in Table A2.1.

Table A2.1 Comparison among DeepLabCut networks. This includes how accurate each DeepLabCut network was with varying manually annotated frames and unique videos. It is generally preferred to have a greater number of unique videos when training deep neural networks [52]. The final two networks described in this table are the same ones described in the Methods and Results sections of Chapter 2.

Network	Test Pixel Error	Frames Manually Annotated	Unique Videos
Nonhuman primate SCI side (multi-animal)	22.51	1344	64
Nonhuman primate Z	40.92	236	4
Nonhuman primate Z2	25.39	132	3
Nonhuman primate SCI top V	15.8	400	25
Nonhuman primate SCI side P	11.25	400	25
Nonhuman primate SCI side F	11.78	450	18
Nonhuman primate 2 animal Unimpaired Side	15.66	456	12
Nonhuman primate 2 animal Unimpaired Top	24.31	456	12

When comparing the test pixel errors against each other, the error rate is relatively stable with the exception of Nonhuman primate Z. This would suggest that there could be a limitation with the tracking using DeepLabCut. To investigate further, a normalized method of comparison was used. This comparison used the percent difference instead of the test pixel error, which is defined by the following equation.

$$\text{Test Pixel error/Minimum Recording Resolution axis} \qquad \text{(Eq. 1)}$$

This equation assumes that the test pixel error occurs in the smaller of the two recording axes. This results in the maximum error possible as it assumes that the entire error occurs in the smaller axis [59]. Additionally, this eliminates the effect of recording at higher resolutions which have more pixels at large. These results of this analysis are shown in Table A2.2.

Table A2.2. Comparison of percent pixel difference among DeepLabCut networks			
Network	Test Pixel Error	Smallest Resolution Axis	Percent Pixel Difference
Reference DeepLabCut network	3	480	0.625
Nonhuman primate SCI side (multi-animal)	22.51	1080	2.08
Nonhuman primate Z	40.92	1080	3.79
Nonhuman primate Z2	25.39	1080	2.35
Nonhuman primate SCI top (V)	15.8	1080	1.46
Nonhuman primate SCI side (P)	11.25	1080	1.04
Nonhuman primate SCI side (F)	11.78	1080	1.09
Nonhuman primate 2 animal Unimpaired Side	15.66	1080	1.45
Nonhuman primate 2 animal Unimpaired Top	24.31	1080	2.25

This comparison shows that the difference between the average reference DeepLabCut network using 400 annotated frames and the nonhuman primate DeepLabCut networks are more aligned. A higher percent pixel difference still persists in the nonhuman primate DeepLabCut networks. One explanation could be user error, and errors when manually annotating frames. This would lead to higher pixel errors as the network is incorrectly trained. It is generally accepted that a neural network is only as accurate as the information that it is given [70]. One previously cited reasoning discusses the movement in and out of frame whereas the original DeepLabCut trained networks have the desired tracked locations always in frame [63]. This would reduce the predictability of the location's movement. Another possible explanation is the rapid movement during the Brinkman board task and the motion blur associated with the task discussed previously.